Two-Microphone Hearing Aids Using Prediction Error Method for Adaptive Feedback Control

Linh Thi Thuc Tran, *Student Member, IEEE*, Sven Erik Nordholm, *Senior Member, IEEE*, Henning Schepker, *Student Member, IEEE*, Hai Huyen Dam, and Simon Doclo, *Senior Member, IEEE*

***Abstract*—A challenge in hearing aids is adaptive feedback control which often uses an adaptive filter to estimate the feedback path. This estimate of the feedback path usually results in a bias due to the correlation between the loudspeaker signal and the incoming signal. The prediction error method (PEM) is a popular method for reducing this bias for adaptive feedback control (AFC) in hearing aids, providing a significant performance improvement compared to conventional adaptive feedback control techniques. However, the PEM-based AFC (PEM-AFC) applications are still limited to single-microphone single-loudspeaker (SMSL) systems. This paper investigates the application of the PEM-AFC to a two-microphone single-loudspeaker hearing aid with detailed theoretical analysis as well as practical experiments. In the proposed method, PEM-AFC2, we use the two-microphone adaptive feedback control (AFC2) method with two microphones and one loudspeaker. The incoming signals at the two microphones are related by a relative transfer function (RTF) which is used to predict the incoming signal at the main microphone. In addition, a prefilter is employed to prewhiten the loudspeaker and the microphone signals before the adaptive filter estimates. As a result, the proposed method obtains a lower bias and a faster tracking rate compared to the PEM-AFC and the AFC2 method, while still maintaining a good quality of the incoming signal. A new derivation for optimal filters in the AFC2 method will also be provided. The performance of the proposed method is evaluated for speech shaped noise as incoming signal and with undermodeling the RTF as well as with perfect modeling the RTF. Moreover, different types of incoming signals and a sudden change of feedback paths are also considered. The experimental results show that the proposed approach yields a significant performance improvement compared to existing state-of-the-art AFC methods such as the PEM-AFC and the AFC2.**

***Index Terms*—Adaptive feedback control, prediction error method, misalignment, added stable gain, AFC2, PEM-AFC2.**

Manuscript received August 16, 2017; revised December 4, 2017 and January 10, 2018; accepted January 17, 2018. Date of publication January 26, 2018; date of current version March 15, 2018. The associate editor coordinating the review of this manuscript and approving it for publication was Prof. Tan Lee. *(Corresponding author: Linh Thi Thuc Tran.)*

L. T. T. Tran and S. E. Nordholm are with the Department of Electrical and Computer Engineering, Curtin University, Perth, WA 6845, Australia (e-mail: t.tran57@postgrad.curtin.edu.au; S.Nordholm@curtin.edu.au).

S. Doclo and H. Schepker are with the Department of Medical Physics and Acoustics and the Cluster of Excellence "Hearing4All", University of Oldenburg, Oldenburg 26129, Germany (e-mail: simon.doclo@uni-oldenburg.de; henning.schepker@uni-oldenburg.de).

H. H. Dam is with the Department of Mathematics and Statistics, Curtin University, Perth, WA 6845, Australia (e-mail: H.Dam@exchange.curtin.edu.au).

Color versions of one or more of the figures in this paper are available online at http://ieeexplore.ieee.org.

Digital Object Identifier 10.1109/TASLP.2018.2798822

I. Introduction

HEARING aids (HAs) are subject to acoustic feedback produced by the loudspeaker signal coupling into the microphone. The feedback signal is amplified and looped back into the loudspeaker, forming a closed loop system. This inherent part of hearing aids limits their achievable amplification and decreases the signal quality. Under some circumstances, this closed feedback loop causes "howling" to the system. The feedback problem becomes more and more challenging with an increased demand for open fittings as well as a decrease in the size of hearing aids. During the last decades many adaptive feedback control (AFC) methods have been introduced [1]–[3]. In conventional AFC methods using single-microphone single-loudspeaker (SMSL), an adaptive filter is employed to estimate the acoustic feedback path. The estimated feedback signal is computed by using the estimated feedback path, which is then subtracted from the microphone signal (cf. Fig. 1). However, the feedback estimate often has a large bias [1], [2], [4] due to the possible strong correlation between the loudspeaker signal and the incoming signal, in particular when the incoming signal is spectrally colored like speech, tones, music, etc. To address the bias problem, many decorrelation approaches have been introduced for AFC such as inserting a delay [1], [5], using frequency shifting [6], [7], phase modulation [8], inserting a probe signal [9]–[12], or employing pre-filters [13], [14]. Among these methods, the PEM-based AFC (PEM-AFC) appears to be a dominant method for SMSL hearing aids, both in time domain [14]–[19] as well as in frequency domain [20]–[23]. The main idea of this method is to filter the input signals of the adaptive filter by prewhitening filters. Thus, the bias in estimation of the feedback path can be reduced significantly due to the lower correlation between the incoming and the loudspeaker signals.

Recently, several methods for adaptive feedback control using multiple microphones and single loudspeaker (MMSL) have been proposed in the literature for public address (PA) applications [24], [25] as well as for HA applications [11], [26]–[29]. In those methods, a beamformer was used to reduce the acoustic feedback. A new approach for adaptive feedback control using two microphones for hearing aids (AFC2) was introduced in [30], [31]. In this approach, the first (main) microphone signal was related to the second microphone signal by a relative transfer function (RTF). The estimated RTF and the second microphone signal were employed to estimate an incoming signal. Note that the second microphone was spatially placed farther away from

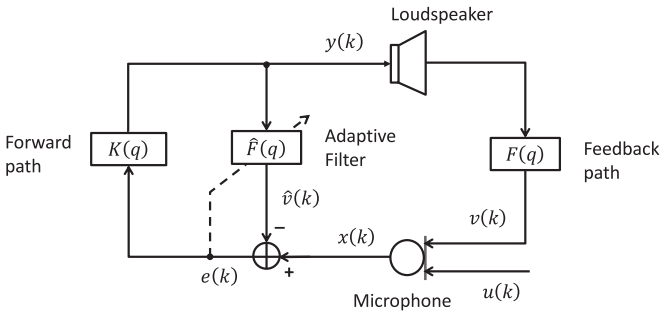

Fig. 1. Conventional AFC model.

the loudspeaker compared to the first microphone such that the second feedback channel had much weaker coupling. Then the estimated incoming signal was used to compute the error signal utilized to control the adaptive filters. By eliminating the contribution of the incoming signal in the adaptation of adaptive filters, a lower bias can be achieved. The AFC2 method provides a significant improvement compared to the PEM-AFC regarding maximum stable gain (MSG) and misalignment (MIS) as well as a stable steady-state solution for varying input signals [31]. Some variants of the AFC2 method have been studied to obtain further performance improvement, such as implementing transform domain processing [32], variable step-size affine projection algorithm [33], proportionate algorithms [34] and sub-band techniques [35].

In this paper, we first consider the SMSL AFC approaches such as the conventional AFC method and the PEM-AFC. Then the MMSL AFC approaches, in particular here the AFC2 method and the proposed method will be mentioned. In fact, we provide a new derivation for the AFC2 method. This is an essential work, since we found that there was an inherent mathematical problem in the "so-called" optimal solution in [31]. In addition, we propose to combine the PEM [14] and the AFC2 method, forming a new method called the PEM-AFC2. The proposed PEM-AFC2 is theoretically analyzed to show that it obtains a lower bias compared to the AFC2 method due to the adaptive pre-whitening of the filter's inputs. Furthermore, we evaluate the performance of the proposed method in comparison with those of the PEM-AFC and the AFC2 method. The experimental results show that in fact the PEM-AFC2 achieves significant misalignment and added stable gain (ASG) improvements compared to the PEM-AFC [14] and the AFC2 method [30], [31] for music as well as different types of speech as the incoming signals and with/without a sudden change of feedback paths. Especially, when the incoming signals are speech shaped noise (SSN), the proposed method yields a better solution for both identifications of the feedback path and the relative transfer function (RTF) compared to the AFC2 method in the case of undermodeling the RTF. For the case of perfect modeling the RTF, both the proposed method and the AFC2 method achieve a unbiased solution for the identification of the RTF and the same solution for the identification of the feedback path.

Throughout this paper, vectors and matrices are emphasized using lower and upper letters in bold, respectively. $E\{.\}$ denotes the expectation operation and the superscript T denotes transposition. The auto-correlation matrix of a vector $\mathbf{m}$, the cross-correlation matrix between two vectors $\mathbf{m}$ and $\mathbf{n}$, and the cross-correlation vector between a vector $\mathbf{m}$ and a scalar ς are represented by $\boldsymbol{R}_{\mathbf{m}}$, $\boldsymbol{R}_{\mathbf{mn}}$ and $\boldsymbol{r}_{\mathbf{m}\varsigma}$, respectively, i.e., $\boldsymbol{R}_{\mathbf{m}} = E\{\mathbf{m}\mathbf{m}^T\}$, $\boldsymbol{R}_{\mathbf{mn}} = E\{\mathbf{m}\mathbf{n}^T\}$, and $\boldsymbol{r}_{\mathbf{m}\varsigma} = E\{\mathbf{m}\varsigma\}$.

The paper is organized as follows. Sections II and III review the conventional AFC method and the PEM-AFC, respectively. A new derivation for optimal filters in the AFC2 model is described in Section IV-C. Section V theoretically analyses the proposed PEM-AFC2 in detail. Experimental results are shown in Section VI. Section VII provides a computational complexity analysis of the proposed method in comparison with the PEM-AFC and the AFC2 method. Section VIII concludes the paper.

II. AFC MODEL

Fig. 1 shows a SMSL adaptive feedback control system. For simplicity, in this paper we assume that all AFC systems are discrete-time, linear time-invariant and that the incoming signal is stationary.

The microphone signal consists of two contributions, namely the incoming signal $u(k)$ and the feedback contribution $v(k) = \mathbf{f}^T\mathbf{y}(k)$ due to the coupling between the loudspeaker and the microphone signals, i.e.,

$$x(k) = u(k) + \mathbf{f}^T\mathbf{y}(k), \tag{1}$$

where k is the discrete-time index, and $\mathbf{y}(k) = [y(k), y(k-1), \ldots, y(k-L_f+1)]^T$ is a vector of the loudspeaker signal of length L_f. The filter $\mathbf{f} = [f_0, f_1, \ldots, f_{L_f-1}]^T$ is the true feedback path vector of length L_f, which can be represented as a polynomial transfer function in q, i.e., $F(q) = \mathbf{f}^T\mathbf{q}$, where $\mathbf{q} = [1 \quad q^{-1} \quad \ldots \quad q^{-L_f+1}]^T$. In this system, the feedback path is first estimated by using an adaptive filter, then the estimated feedback path is used to compute the estimated feedback contribution $\hat{v}(k)$ which is subtracted from the microphone signal $x(k)$, producing an error signal $e(k)$. This error signal is utilized for the adaptive estimate of the feedback path and computed as

$$e(k) = x(k) - \hat{v}(k), \tag{2}$$

where $\hat{v}(k) = \hat{\mathbf{f}}^T\mathbf{y}(k)$ is an estimate of the feedback signal with a $L_{\hat{f}}$-dimensional vector $\mathbf{y}(k)$ and $\hat{\mathbf{f}} = [\hat{f}_0, \hat{f}_1, \ldots, \hat{f}_{L_{\hat{f}}-1}]^T$ is the estimated feedback path of length $L_{\hat{f}}$. The loudspeaker signal is equal to the error signal processed by the forward path $K(q)$ of the hearing aids, i.e.,

$$y(k) = K(q)\,e(k). \tag{3}$$

In this paper we assume that $K(q) = q^{-d_k}|K|$, where $d_k \geqslant 1$ and $|K|$ represent the delay and the gain in the forward path, respectively.

We minimize the the cost function $J\left(\hat{\mathbf{f}}\right) = E\{e^2(k)\}$ with respect to $\hat{\mathbf{f}}$, in order to obtain the optimal solution

$$\hat{\mathbf{f}}_0 = E\{\mathbf{y}(k)\mathbf{y}^T(k)\}^{-1}E\{\mathbf{y}(k)x(k)\}. \tag{4}$$

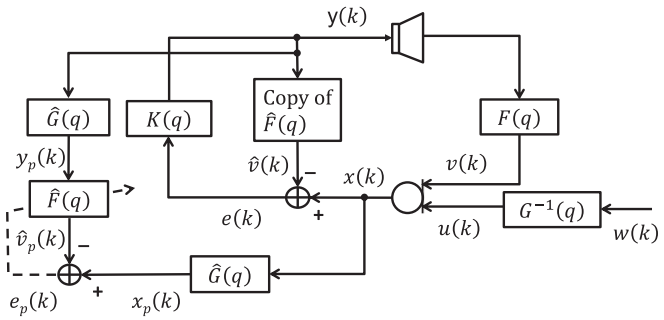

Fig. 2. PEM-AFC model.

By substituting (1) into (4), we achieve [1]

$$\hat{\mathbf{f}}_0 = \mathbf{f} + \underbrace{\boldsymbol{R}_{\mathbf{y}}^{-1}\boldsymbol{r}_{\mathbf{y}u}}_{\text{bias}}. \tag{5}$$

It can be seen that the estimate of the feedback path in (5) includes a bias which depends on the correlation between the loudspeaker and incoming signals, i.e., the incoming signal behaves as a disturbance to the feedback canceler [2].

The optimal weight vector $\hat{\mathbf{f}}_0$ is approximated recursively using the NLMS algorithm as follows

$$\hat{\mathbf{f}}\,(k) = \hat{\mathbf{f}}\,(k-1) + \frac{\mu}{\mathbf{y}^T\,(k)\,\mathbf{y}\,(k) + \delta}\mathbf{y}\,(k)\,e\,(k)\,, \tag{6}$$

where μ is a step-size and δ is a small positive value added to avoid division by zero.

III. PEM-AFC

To reduce the bias in the estimation of the feedback path, pre-filters are used to pre-whiten the inputs of the adaptive filter in the PEM-AFC. Fig. 2 depicts an AFC model using the PEM for a SMSL hearing aid [2], [14], [20]. In the PEM-AFC, the incoming signal is assumed to be modeled by an auto-regressive (AR) process, i.e.,

$$u\,(k) = G^{-1}\,(q)\,w\,(k)\,, \tag{7}$$

where $G^{-1}\,(q)$ is a monic and inversely stable all-pole filter and $w\,(k)$ is a white Gaussian noise sequence. The estimated filter $\hat{G}\,(q)$ of $G\,(q)$ is used to pre-whiten the loudspeaker and microphone signals,

$$x_p\,(k) = \hat{G}\,(q)\,x\,(k)\,, \tag{8}$$

$$y_p\,(k) = \hat{G}\,(q)\,y\,(k)\,. \tag{9}$$

The prediction error signal $e_p\,(k)$ is calculated by subtracting the pre-whitened estimation of feedback signal from the pre-whitened microphone signal as

$$e_p\,(k) = x_p\,(k) - \hat{\mathbf{f}}^T\mathbf{y}_p\,(k)\,, \tag{10}$$

where $\mathbf{y}_p(k) = [y_p(k), y_p(k-1), \ldots, y_p(k-L_{\hat{f}}+1)]^T$ is a $L_{\hat{f}}$-dimensional vector. By minimizing the mean square prediction error, $E\left\{e_p^2\,(k)\right\}$, the optimal weight vector for the estimated feedback path in the PEM-AFC is equal to

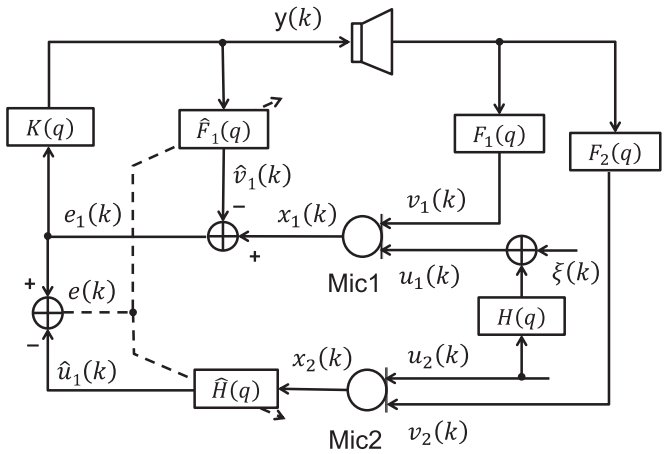

Fig. 3. AFC2 model.

$$\hat{\mathbf{f}}_0 = E\left\{\mathbf{y}_p\,(k)\,\mathbf{y}_p^T\,(k)\right\}^{-1}E\left\{\mathbf{y}_p\,(k)\,x_p\,(k)\right\}, \tag{11}$$

$$\hat{\mathbf{f}}_0 = \mathbf{f} + \underbrace{\boldsymbol{R}_{\mathbf{y}_p}^{-1}\boldsymbol{r}_{\mathbf{y}_p u_p}}_{\text{bias}}, \tag{12}$$

where $u_p\,(k)$ is denoted as

$$u_p\,(k) = \hat{G}\,(q)\,u\,(k)\,. \tag{13}$$

Substitute (7) and (13) into (12), it can be seen that an unbiased solution for estimation of the feedback path can be achieved if $\hat{G}\,(q) = G\,(q)$, the assumption (7) is satisfied and there is at least one delay in the forward path. Moreover, if the delay in the forward path is not smaller than the length of AR model $\hat{G}\,(q)$, both the feedback path $F\,(q)$ and the AR model $\hat{G}\,(q)$ can be identified in closed-loop without adding a probe signal or nonlinearities [2], [14].

For the PEM-AFC, the optimal coefficients $\hat{\mathbf{f}}_0$ are recursively updated as follows

$$\hat{\mathbf{f}}\,(k) = \hat{\mathbf{f}}\,(k-1) + \frac{\mu}{\mathbf{y}_p^T\,(k)\,\mathbf{y}_p\,(k) + \delta}\mathbf{y}_p\,(k)\,e_p\,(k)\,, \tag{14}$$

with $e_p\,(k)$ defined in (10).

IV. New Insights Into AFC2 Method

A. AFC2 Model

In this subsection, the structure of the AFC system using two microphones and one loudspeaker, which was introduced in [31], is briefly reviewed. Fig. 3 illustrates the AFC2 model, in which the main microphone is located in the ear canal (Mic1) and the second microphone (Mic2) is placed behind the ear. The loudspeaker is placed near the main microphone (Mic1). The distance between the two microphones needs to be far enough to ensure that the second feedback signal is more attenuated than the first feedback signal [30], [31]. Each microphone receives the incoming signal from the surrounding environment as well

as a feedback signal, i.e.,

$$x_1(k) = u_1(k) + \mathbf{f}_1^T \mathbf{y}(k), \tag{15}$$

$$x_2(k) = u_2(k) + \mathbf{f}_2^T \mathbf{y}(k), \tag{16}$$

where $\mathbf{f}_i = [f_{i,0}, f_{i,1}, \ldots, f_{i,L_f-1}]^T$ with $i = 1, 2$ is a FIR filter of length L_f modeling the ith acoustic feedback path; $\mathbf{y}(k)$ is the loudspeaker signal vector of length L_f and $u_i(k)$ is the incoming signal received at the ith microphone. The filter $\mathbf{f}_i$ is represented as $F_i(q) = \mathbf{f}_i^T \mathbf{q}$. Assuming that the incoming signals at the two microphones are related as

$$u_1(k) = \mathbf{h}^T \mathbf{u}_2(k) + \xi(k), \tag{17}$$

where $\mathbf{h} = [h_0, h_1, \ldots, h_{L_h-1}]^T$ is the impulse response of the relative transfer function (RTF) $H(q)$ of length L_h and $\xi(k)$ is the residual error caused by undermodeling the RTF. We assume that $\mathbf{h}$ is causal due to the positioning arrangement of the microphones.

The two-microphone method is based on the idea that the second microphone provides additional information. This information is utilized to estimate the first incoming signal $u_1(k)$ which is then subtracted from the error signal $e_1(k)$, forming a new error signal $e(k)$, i.e.,

$$e(k) = e_1(k) - \hat{u}_1(k), \tag{18}$$

where

$$\begin{aligned} e_1(k) &= x_1(k) - \hat{v}_1(k) \\ &= u_1(k) + \left(\mathbf{f}_1^T - \hat{\mathbf{f}}_1^T\right)\mathbf{y}(k), \end{aligned} \tag{19}$$

and

$$\hat{u}_1(k) = \hat{\mathbf{h}}^T \mathbf{x}_2(k), \tag{20}$$

where $\hat{\mathbf{f}}_1$ is the estimate of $\mathbf{f}_1$, $\hat{v}_1(k) = \hat{\mathbf{f}}_1^T \mathbf{y}(k)$ is the output of the feedback canceler, $\hat{\mathbf{h}} = [\hat{h}_0, \hat{h}_1, \ldots, \hat{h}_{L_{\hat{h}}-1}]^T$ is a vector of length $L_{\hat{h}}$ representing the IR of the FIR filter $\hat{H}(q)$ used to identify $H(q)$, and $\mathbf{x}_2(k)$ is a $L_{\hat{h}}$-dimensional vector denoting the second microphone signal, $\mathbf{x}_2(k) = [x_2(k), x_2(k-1), \ldots, x_2(k - L_{\hat{h}} + 1)]^T$.

The error signal $e(k)$ is used to control the adaptation processes of both $\hat{F}_1(q)$ and $\hat{H}(q)$, resulting in lower bias terms [31]. The loudspeaker signal is equal to

$$y(k) = K(q)\, e_1(k). \tag{21}$$

B. Derivation Problem

In this subsection, the theoretical analysis for the AFC2 method, which was derived in [31], is briefly reviewed. We show that the "so-called" optimal solution in [31] is in fact not an optimal solution due to the dependency on $\hat{\mathbf{h}}$.

By substituting (20), (19), (17), and (16) into (18), we obtain

$$\begin{aligned} e(k) &= \left(\mathbf{f}_1^T - \hat{\mathbf{f}}_1^T\right)\mathbf{y}(k) + \left(\mathbf{h}^T - \hat{\mathbf{h}}^T\right)\mathbf{u}_2(k) \\ &\quad - \mathbf{f}_{2_{\hat{\mathbf{h}}}}^T \mathbf{y}(k) + \xi(k) \\ &= \overline{\mathbf{f}}_1^T \mathbf{y}(k) + \overline{\mathbf{h}}^T \mathbf{u}_2(k) - \mathbf{f}_{2_{\hat{\mathbf{h}}}}^T \mathbf{y}(k) + \xi(k), \end{aligned} \tag{22}$$

where $\overline{\mathbf{f}}_1 = \mathbf{f}_1 - \hat{\mathbf{f}}_1$, $\overline{\mathbf{h}} = \mathbf{h} - \hat{\mathbf{h}}$ and $\mathbf{f}_{2_{\hat{\mathbf{h}}}} = [f_{2_{\hat{\mathbf{h}},0}}, \ldots, f_{2_{\hat{\mathbf{h}},L_f-1}}]^T$ is the coefficient vector of $\hat{H}(q)F_2(q)$.

Let $\mathbf{x}(k) = [\mathbf{y}^T(k)\ \mathbf{u}_2^T(k)]^T$, $\mathbf{z}(k) = [\mathbf{y}^T(k)\ \mathbf{0}^T]^T$, and the vectors $\overline{\mathbf{a}}$ and $\overline{\mathbf{b}}$ be defined as

$$\overline{\mathbf{a}} = \left[\overline{\mathbf{f}}_1^T\ \ \overline{\mathbf{h}}^T\right]^T, \tag{23}$$

$$\overline{\mathbf{b}} = \left[\mathbf{f}_{2_{\hat{\mathbf{h}}}}^T\ \ \mathbf{0}^T\right]^T, \tag{24}$$

where the null vectors have the dimension of $L_{\hat{h}}$.

Then the error signal $e(k)$ can be reformulated as

$$e(k) = \overline{\mathbf{a}}^T \mathbf{x}(k) - \overline{\mathbf{b}}^T \mathbf{z}(k) + \xi(k). \tag{25}$$

Minimizing the cost function $J(\overline{\mathbf{a}}) = E\{e^2(k)\}$ with respect to $\overline{\mathbf{a}}$ results in the following "so-called" optimal solution

$$\overline{\mathbf{a}}_o = \begin{bmatrix} \overline{\mathbf{f}}_{1_o} \\ \overline{\mathbf{h}}_o \end{bmatrix} = \boldsymbol{R}_{\mathbf{x}}^{-1} \boldsymbol{R}_{\mathbf{xz}} \overline{\mathbf{b}} - \boldsymbol{R}_{\mathbf{x}}^{-1} \boldsymbol{r}_{\mathbf{x}\xi}. \tag{26}$$

As we can see from (23) and (24), the term $\hat{\mathbf{h}}$ appeared in both the $\overline{\mathbf{a}}$ and $\overline{\mathbf{b}}$ terms, so that the "so-called" optimal solution for $\min_{\overline{\mathbf{a}}}\{E\{e^2(k)\}\}$ received in (26) was not a correct solution for $\overline{\mathbf{a}}$.

C. New Derivation for AFC2 Method

To address the above derivation problem inherited from [31], we provide a new derivation for the AFC2 in the following.

Considering that $\xi(k)$ is the residual error caused by undermodeling the RTF ($\xi(k) \neq 0$), we define

$$\xi(k) = \mathbf{h}_{\text{res}}^T \mathbf{u}_2(k), \tag{27}$$

where $\mathbf{h}_{\text{res}} = [\underbrace{0, \ldots, 0}_{L_h}, h_{L_h}, \ldots, h_{L_{h_{\text{full}}}-1}]^T$ is the impulse response of $H_{\text{res}}(q)$. The full RTF has impulse response $\mathbf{h}_{\text{full}} = \mathbf{h} + \mathbf{h}_{\text{res}}$, where $\mathbf{h} = [h_0, \ldots, h_{L_h-1}, \underbrace{0, \ldots, 0}_{L_{h_{\text{full}}} - L_h}]^T$, $L_{h_{\text{full}}}$ is the length of $\mathbf{h}_{\text{full}}$. The vector $\hat{\mathbf{h}}$ is now defined as $\hat{\mathbf{h}} = [\hat{h}_0, \ldots, \hat{h}_{L_{\hat{h}}-1}, \underbrace{0, \ldots, 0}_{L_{h_{\text{full}}} - L_{\hat{h}}}]^T$ with $L_{\hat{h}} = L_h$.

In the new derivation the error signal $e(k)$ can be obtained by substituting (17), (19), and (20) into (18), i.e.,

$$\begin{aligned} e(k) &= \mathbf{h}^T \mathbf{u}_2(k) + \xi(k) + \left(\mathbf{f}_1^T - \hat{\mathbf{f}}_1^T\right)\mathbf{y}(k) \\ &\quad - \hat{\mathbf{h}}^T \mathbf{x}_2(k), \end{aligned} \tag{28}$$

where $\mathbf{u}_2(k)$ and $\mathbf{x}_2(k)$ are defined in a manner analogous to those described in subsection IV-A but with the length $L_{h_{\text{full}}}$.

Let $\mathbf{a} = [\hat{\mathbf{f}}_1^T\ \hat{\mathbf{h}}^T]^T$, $\mathbf{b} = [\mathbf{f}_1^T\ \mathbf{h}^T]^T$, $\mathbf{z}_1(k) = [\mathbf{y}^T(k)\ \mathbf{x}_2^T(k)]^T$, and $\mathbf{z}_2(k) = [\mathbf{y}^T(k)\ \mathbf{u}_2^T(k)]^T$. The cost function is now defined as

$$\begin{aligned} J(\mathbf{a}) &= E\left\{e^2(k)\right\} \\ &= E\left\{\left[\mathbf{a}^T \mathbf{z}_1(k) - \left(\mathbf{b}^T \mathbf{z}_2(k) + \xi(k)\right)\right]^2\right\}. \end{aligned} \tag{29}$$

Minimizing the cost function in (29) with respect to $\mathbf{a}$, we obtain the optimal solution

$$\mathbf{a}_o = \begin{bmatrix} \hat{\mathbf{f}}_{1_o} \\ \widehat{\mathbf{h}}_o \end{bmatrix} = \boldsymbol{R}_{\mathbf{z}_1}^{-1} \boldsymbol{R}_{\mathbf{z}_1 \mathbf{z}_2} \mathbf{b} + \boldsymbol{R}_{\mathbf{z}_1}^{-1} \boldsymbol{r}_{\mathbf{z}_1 \xi}. \tag{30}$$

The derivations for computing the terms $\boldsymbol{R}_{\mathbf{z}_1}^{-1} \boldsymbol{R}_{\mathbf{z}_1 \mathbf{z}_2} \mathbf{b}$ and $\boldsymbol{R}_{\mathbf{z}_1}^{-1} \boldsymbol{r}_{\mathbf{z}_1 \xi}$ are outlined in Appendix A. Hence,

$$\boldsymbol{R}_{\mathbf{z}_1}^{-1} \boldsymbol{R}_{\mathbf{z}_1 \mathbf{z}_2} \mathbf{b} = \begin{bmatrix} \mathbf{f}_1 - \mathbf{f}_{2_\mathbf{h}} \\ \mathbf{h} \end{bmatrix}, \tag{31}$$

$$\boldsymbol{R}_{\mathbf{z}_1}^{-1} \boldsymbol{r}_{\mathbf{z}_1 \xi} = \begin{bmatrix} \boldsymbol{B}_1 \\ \boldsymbol{B}_\mathbf{h} \end{bmatrix}, \tag{32}$$

where $\mathbf{f}_{2_\mathbf{h}}$ is a coefficient vector of the product $H(q) F_2(q)$ and

$$\boldsymbol{B}_\mathbf{h} = \boldsymbol{N}^T \boldsymbol{r}_{\mathbf{y}\xi} + \boldsymbol{Q} \boldsymbol{r}_{\mathbf{x}_2 \xi}, \tag{33}$$

$$\boldsymbol{B}_1 = \boldsymbol{R}_\mathbf{y}^{-1} \boldsymbol{r}_{\mathbf{y}\xi} + \left(\boldsymbol{N} \boldsymbol{r}_{\mathbf{x}_2 \xi} - \boldsymbol{N} \boldsymbol{R}_{\mathbf{x}_2 \mathbf{y}} \boldsymbol{R}_\mathbf{y}^{-1} \boldsymbol{r}_{\mathbf{y}\xi} \right), \tag{34}$$

with $\boldsymbol{N} = -\boldsymbol{R}_\mathbf{y}^{-1} \boldsymbol{R}_{\mathbf{y}\mathbf{x}_2} \left(\boldsymbol{R}_{\mathbf{x}_2} - \boldsymbol{R}_{\mathbf{x}_2 \mathbf{y}} \boldsymbol{R}_\mathbf{y}^{-1} \boldsymbol{R}_{\mathbf{y}\mathbf{x}_2} \right)^{-1}$, $\boldsymbol{Q} = (\boldsymbol{R}_{\mathbf{x}_2} - \boldsymbol{R}_{\mathbf{x}_2 \mathbf{y}} \boldsymbol{R}_\mathbf{y}^{-1} \boldsymbol{R}_{\mathbf{y}\mathbf{x}_2})^{-1}$.

Therefore, the optimal solution in (30) can be rewritten as

$$\hat{\mathbf{f}}_{1_o} = \mathbf{f}_1 - \mathbf{f}_{2_\mathbf{h}} + \boldsymbol{B}_1, \tag{35}$$

$$\widehat{\mathbf{h}}_o = \mathbf{h} + \boldsymbol{B}_\mathbf{h}. \tag{36}$$

For perfect modeling case, $\xi(k) = 0$, hence $\boldsymbol{r}_{\mathbf{y}\xi} = \boldsymbol{r}_{\mathbf{x}_2 \xi} = \mathbf{0}$. The (33)–(36) can be reformulated as

$$\boldsymbol{B}_\mathbf{h} = \mathbf{0}, \tag{37}$$

$$\boldsymbol{B}_1 = \mathbf{0}, \tag{38}$$

$$\hat{\mathbf{f}}_{1_o} = \mathbf{f}_1 - \mathbf{f}_{2_\mathbf{h}}, \tag{39}$$

$$\widehat{\mathbf{h}}_o = \mathbf{h}. \tag{40}$$

In this case, there is no bias in the estimate of $H(q)$ and the accuracy in identification of $F_1(q)$ now only depends on the value of $\mathbf{f}_{2_\mathbf{h}}$. Thus, if the second feedback path $\mathbf{f}_2$ is weak compared to the first feedback path due to their assigned positions, i.e., $\mathbf{f}_2 \approx \mathbf{0}$, an unbiased estimate may be obtained. In practice, it's not possible to have $\mathbf{f}_2 \approx \mathbf{0}$ since the distance between the loudspeaker and the second microphone could not be too far due to the small size of a hearing aid. Moreover, $\xi(k)$ is usually not zero as well.

In the AFC2 method, the optimal weight vectors $\hat{\mathbf{f}}_{1_o}$, $\widehat{\mathbf{h}}_o$ in (30) are recursively estimated as follows

$$\hat{\mathbf{f}}_1(k) = \hat{\mathbf{f}}_1(k-1) + \frac{\mu}{\mathbf{y}^T(k)\mathbf{y}(k) + \delta} \mathbf{y}(k) e(k), \tag{41}$$

$$\hat{\mathbf{h}}(k) = \hat{\mathbf{h}}(k-1) + \frac{\mu}{\mathbf{x}_2^T(k)\mathbf{x}_2(k) + \delta} \mathbf{x}_2(k) e(k), \tag{42}$$

with $e(k)$ defined in (28).

V. Proposed PEM-AFC2

The proposed PEM-AFC2 is based on the combination of two state-of-the-art methods, the PEM-AFC and the AFC2. As a result, the proposed method improves the state-of-the-art methods in terms of a lower bias and a faster tracking rate, while maintaining a good signal quality for both music and speech incoming signals. This section provides the theoretical analysis of the PEM-AFC2 in detail. This analysis is inspired from the derivation of the PEM-AFC in Section III and the new derivation of the AFC2 in subsection IV-C. We show that by pre-whitening the inputs of adaptive filters in the AFC2 method, the bias terms in the identifications of the feedback channel $F_1(q)$ and the RTF $H(q)$ can be significantly reduced.

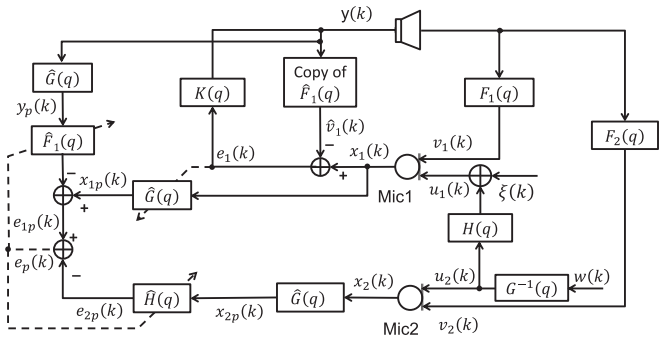

Fig. 4. PEM-AFC2 model.

Fig. 4 illustrates the proposed PEM-AFC2 model. We assume that the second incoming signal $u_2(k)$ can be modeled as follows

$$u_2(k) = G^{-1}(q) w(k), \tag{43}$$

where $w(k)$ is a zero-mean, white Gaussian noise sequence and $G^{-1}(q)$ is a monic and inversely stable all-pole filter.

The loudspeaker and microphone signals are pre-whitened by $\hat{G}(q)$ which is an estimate of $G(q)$, before they are fed into adaptive filters. The pre-whitened error signal can be calculated as

$$e_p(k) = e_{1p}(k) - e_{2p}(k), \tag{44}$$

where $e_{1p}(k) = x_{1p}(k) - \hat{F}_1(q) y_p(k)$ and $e_{2p}(k) = \hat{H}(q) x_{2p}(k)$. The pre-whitened microphone and loudspeaker signals are defined as

$$x_{1p}(k) = \hat{G}(q) x_1(k), \tag{45}$$

$$x_{2p}(k) = \hat{G}(q) x_2(k), \tag{46}$$

$$y_p(k) = \hat{G}(q) y(k). \tag{47}$$

The error signal $e_p(k)$ is used to control the adaptive process in filters $\hat{F}_1(q)$ and $\hat{H}(q)$. By substituting (15) and (17) into (45) we can reformulate the pre-whitened first microphone signal $x_{1p}(k)$ as follows

$$\begin{aligned} x_{1p}(k) &= \hat{G}(q) \left[u_1(k) + \mathbf{f}_1^T \mathbf{y}(k) \right] \\ &= \mathbf{h}^T \mathbf{u}_{2p}(k) + \xi_p(k) + \mathbf{f}_1^T \mathbf{y}_p(k), \end{aligned} \tag{48}$$

where $\xi_p(k) = \hat{G}(q) \xi(k)$.

Hence, the pre-whitened error signal in (44) can be rewritten as

$$e_p(k) = \mathbf{h}^T \mathbf{u}_{2p}(k) + \xi_p(k) + \left(\mathbf{f}_1^T - \hat{\mathbf{f}}_1^T\right) \mathbf{y}_p(k) - \hat{\mathbf{h}}^T \mathbf{x}_{2p}(k). \quad (49)$$

Assume that the adaptation of $\hat{G}(q)$ is decoupled from the adaptation of $\hat{F}_1(q)$ and $\hat{H}(q)$. The cost function for the PEM-AFC2 is denoted as

$$\begin{aligned} J(\mathbf{a}) &= E\left\{e_p^2(k)\right\} \\ &= E\left\{\left[\mathbf{a}^T \mathbf{z}_{1p}(k) - \left(\mathbf{b}^T \mathbf{z}_{2p}(k) + \xi_p(k)\right)\right]^2\right\}, \end{aligned} \quad (50)$$

where $\mathbf{a}$, $\mathbf{b}$ are defined in a manner analogous to those in subsection IV-C, and $\mathbf{z}_{1p}(k) = \left[\mathbf{y}_p^T(k) \;\; \mathbf{x}_{2p}^T(k)\right]^T$, $\mathbf{z}_{2p}(k) = \left[\mathbf{y}_p^T(k) \;\; \mathbf{u}_{2p}^T(k)\right]^T$.

Minimizing the cost function in (50) with respect to $\mathbf{a}$ results in the optimal solution

$$\mathbf{a}_o = \begin{bmatrix} \hat{\mathbf{f}}_{1_o} \\ \hat{\mathbf{h}}_o \end{bmatrix} = \boldsymbol{R}_{\mathbf{z}_{1p}}^{-1} \boldsymbol{R}_{\mathbf{z}_{1p}\mathbf{z}_{2p}} \mathbf{b} + \boldsymbol{R}_{\mathbf{z}_{1p}}^{-1} \boldsymbol{r}_{\mathbf{z}_{1p}\xi_p}. \quad (51)$$

We derive the terms $\boldsymbol{R}_{\mathbf{z}_{1p}}^{-1} \boldsymbol{R}_{\mathbf{z}_{1p}\mathbf{z}_{2p}} \mathbf{b}$ and $\boldsymbol{R}_{\mathbf{z}_{1p}}^{-1} \boldsymbol{r}_{\mathbf{z}_{1p}\xi_p}$ in a similar way as we have done for $\boldsymbol{R}_{\mathbf{z}_1}^{-1} \boldsymbol{R}_{\mathbf{z}_1\mathbf{z}_2} \mathbf{b}$ and $\boldsymbol{R}_{\mathbf{z}_1}^{-1} \boldsymbol{r}_{\mathbf{z}_1\xi}$ (see Appendix A), hence

$$\boldsymbol{R}_{\mathbf{z}_{1p}}^{-1} \boldsymbol{R}_{\mathbf{z}_{1p}\mathbf{z}_{2p}} \mathbf{b} = \begin{bmatrix} \mathbf{f}_1 - \mathbf{f}_{2_\mathbf{h}} \\ \mathbf{h} \end{bmatrix}, \quad (52)$$

$$\boldsymbol{R}_{\mathbf{z}_{1p}}^{-1} \boldsymbol{r}_{\mathbf{z}_{1p}\xi_p} = \begin{bmatrix} \tilde{\boldsymbol{B}}_1 \\ \tilde{\boldsymbol{B}}_\mathbf{h} \end{bmatrix}, \quad (53)$$

where

$$\tilde{\boldsymbol{B}}_\mathbf{h} = \tilde{\boldsymbol{N}}^T \boldsymbol{r}_{\mathbf{y}_p\xi_p} + \tilde{\boldsymbol{Q}} \boldsymbol{r}_{\mathbf{x}_{2p}\xi_p}, \quad (54)$$

$$\tilde{\boldsymbol{B}}_1 = \boldsymbol{R}_{\mathbf{y}_p}^{-1} \boldsymbol{r}_{\mathbf{y}_p\xi_p} + \left(\tilde{\boldsymbol{N}} \boldsymbol{r}_{\mathbf{x}_{2p}\xi_p} - \tilde{\boldsymbol{N}} \boldsymbol{R}_{\mathbf{x}_{2p}\mathbf{y}_p} \boldsymbol{R}_{\mathbf{y}_p}^{-1} \boldsymbol{r}_{\mathbf{y}_p\xi_p}\right), \quad (55)$$

with $\tilde{\boldsymbol{Q}} = (\boldsymbol{R}_{\mathbf{x}_{2p}} - \boldsymbol{R}_{\mathbf{x}_{2p}\mathbf{y}_p} \boldsymbol{R}_{\mathbf{y}_p}^{-1} \boldsymbol{R}_{\mathbf{y}_p\mathbf{x}_{2p}})^{-1}$, $\tilde{\boldsymbol{N}} = -\boldsymbol{R}_{\mathbf{y}_p}^{-1} \boldsymbol{R}_{\mathbf{y}_p\mathbf{x}_{2p}} \tilde{\boldsymbol{Q}}$.

The derivations in Appendix B show that for undermodeling the RTF we obtain

$$\tilde{\boldsymbol{B}}_\mathbf{h} = \mathbf{h}_{\text{res}}, \quad (56)$$

$$\tilde{\boldsymbol{B}}_1 = -\boldsymbol{R}_{\mathbf{y}_p}^{-1} \boldsymbol{r}_{\mathbf{y}_p\mathbf{x}_{2p}} \mathbf{h}_{\text{res}} = -\boldsymbol{R}_{\mathbf{y}_p}^{-1} \boldsymbol{r}_{\mathbf{y}_p\mathbf{x}_{2p}} \tilde{\boldsymbol{B}}_\mathbf{h}, \quad (57)$$

if the condition $d_k > L_{h_{\text{full}}} - 1$ is satisfied.

Hence, the optimal solution in (51) can be reformulated as

$$\hat{\mathbf{f}}_{1_o} = \mathbf{f}_1 - \mathbf{f}_{2_\mathbf{h}} - \boldsymbol{R}_{\mathbf{y}_p}^{-1} \boldsymbol{r}_{\mathbf{y}_p\mathbf{x}_{2p}} \mathbf{h}_{\text{res}}, \quad (58)$$

$$\hat{\mathbf{h}}_o = \mathbf{h} + \mathbf{h}_{\text{res}}. \quad (59)$$

For the perfect modeling the RTF, $\xi(k) = 0$ (i.e., $\mathbf{h}_{\text{res}} = \mathbf{0}$), we obtain

$$\tilde{\boldsymbol{B}}_\mathbf{h} = \boldsymbol{B}_\mathbf{h} = \mathbf{0}, \quad (60)$$

$$\tilde{\boldsymbol{B}}_1 = \boldsymbol{B}_1 = \mathbf{0}. \quad (61)$$

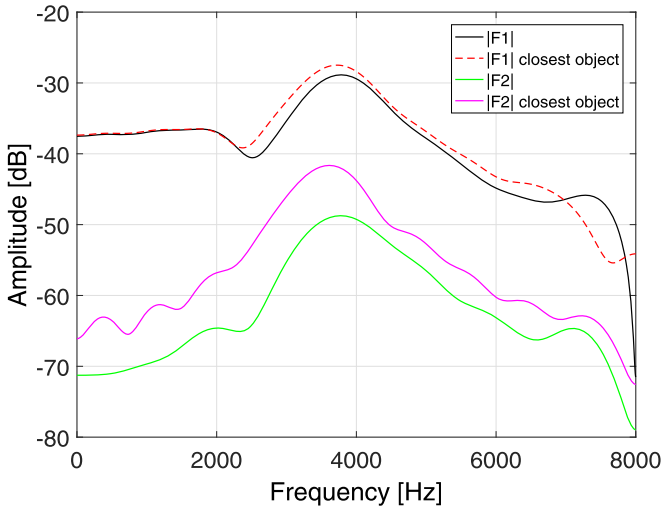

Fig. 5. Amplitude responses of measured feedback paths.

We compare the formula (56) to (33), and see that the proposed PEM-AFC2 results in a better solution for the estimate of $H(q)$ compared to the AFC2 method when $\xi(k) \neq 0$. In fact, in that case the bias in the estimation of $H(q)$ is exactly the residual part $\mathbf{h}_{\text{res}}$ as expected for the PEM-AFC2, but that estimation for the AFC2 method depends on a variety of correlations including $\boldsymbol{R}_\mathbf{y}$, $\boldsymbol{R}_{\mathbf{x}_2}$, $\boldsymbol{R}_{\mathbf{x}_2\mathbf{y}}$, $\boldsymbol{r}_{\mathbf{y}\xi}$ and $\boldsymbol{r}_{\mathbf{x}_2\xi}$. Similarly, from (57) and (34) we see that the PEM-AFC2 also achieve a better solution for the estimation of $F_1(q)$ compared to the AFC2 method.

For the case $\xi(k) = 0$ the PEM-AFC2 and the AFC2 achieve the same bias for the estimates of $H(q)$ and $F_1(q)$ as shown in (60) and (61). In fact, there is no bias for the estimate of $H(q)$ and the estimate of $F_1(q)$ in this case only depends on the value of $\mathbf{f}_{2_\mathbf{h}}$. These conclusions are verified in experimental results (cf. Section VI) which show that the PEM-AFC2 has much better performance than the AFC2 for the case undermodeling the RTF. The reason is that the pre-filters used in the PEM-AFC2 can reduce the bias terms by pre-whitening the inputs of adaptive filters. For the perfect modeling the RTF both methods will converge to the same level with very low steady-state error.

For the PEM-AFC2, the optimal coefficients $\hat{\mathbf{f}}_{1_o}$, $\hat{\mathbf{h}}_o$ in (51) are updated using the NLMS algorithm as follows

$$\hat{\mathbf{f}}_1(k) = \hat{\mathbf{f}}_1(k-1) + \frac{\mu}{\mathbf{y}_p^T(k)\mathbf{y}_p(k) + \delta} \mathbf{y}_p(k) e_p(k), \quad (62)$$

$$\hat{\mathbf{h}}(k) = \hat{\mathbf{h}}(k-1) + \frac{\mu}{\mathbf{x}_{2p}^T(k)\mathbf{x}_{2p}(k) + \delta} \mathbf{x}_{2p}(k) e_p(k), \quad (63)$$

with $e_p(k)$ defined in (44).

VI. Experimental Results

In simulations, measured feedback paths for the case without obstacle between loudspeaker and microphones (namely normal feedback paths) as well as for the case a flat object placed very close to the ear (namely closest feedback paths) have been used [31]. Fig. 5 depicts the amplitude responses of the measured feedback paths. It shows that the closest feedback paths

have higher amplitudes than the corresponding normal feedback paths. The normalized misalignment and added stable gain are used to evaluate the adaptive feedback control methods. The normalized misalignments for estimating $F_1(q)$ (namely MIS) and for estimating $H(q)$ (namely MIS_H) are denoted as [20]

$$\mathrm{MIS} = 10\log_{10}\left(\frac{\int_0^{\pi}\left|F_1\left(e^{j\omega}\right) - e^{-j\omega d_{fb}}\hat{F}_1\left(e^{j\omega}\right)\right|^2 \mathrm{d}\omega}{\int_0^{\pi}\left|F_1\left(e^{j\omega}\right)\right|^2 \mathrm{d}\omega}\right), \tag{64}$$

$$\mathrm{MIS\_H} = 10\log_{10}\left(\frac{\int_0^{\pi}\left|H\left(e^{j\omega}\right) - \hat{H}\left(e^{j\omega}\right)\right|^2 \mathrm{d}\omega}{\int_0^{\pi}\left|H\left(e^{j\omega}\right)\right|^2 \mathrm{d}\omega}\right), \tag{65}$$

and the added stable gain is calculated as [20], [36]

$$\begin{aligned}\mathrm{ASG} = {} & 10\log_{10}\left(\min_{\omega}\frac{1}{\left|F_1\left(e^{j\omega}\right) - e^{-j\omega d_{fb}}\hat{F}_1\left(e^{j\omega}\right)\right|^2}\right) \\ & -10\log_{10}\left(\min_{\omega}\frac{1}{\left|F_1\left(e^{j\omega}\right)\right|^2}\right),\end{aligned} \tag{66}$$

where d_{fb} is a delay in the feedback canceler's path; $F_1\left(e^{j\omega}\right)$ and $\hat{F}_1\left(e^{j\omega}\right)$ are frequency responses of the true and the estimated feedback paths at the normalized angular frequency ω, respectively. We choose the following parameters for all simulations: the delay in the forward path $d_k = 32$ samples, the gain in the forward path $|K| = 30$ dB, the delay in the feedback canceler's path $d_{fb} = 16$ samples, the sampling frequency $f_s = 16$ kHz and $\delta = 10^{-6}$. The lengths of the true and estimated feedback paths are $L_f = 38$ and $L_{\hat{f}} = 22$, respectively. The length $L_h = L_{\hat{h}} = 10$ and $L_{h_{\mathrm{full}}} = 20$ are chosen. For all AFC methods using two microphones, the same step-sizes are chosen to update both adaptive filters $\hat{F}_1(q)$ and $\hat{H}(q)$.

Scenario 1: in this scenario, we use synthesized SSN as the second incoming signal to verify the theoretical analyses for the cases of undermodeling and perfect modeling the RTF. This SSN is generated by passing a white Gaussian noise (WGN) sequence through an all-pole filter $G^{-1}(q)$ with the filter order of 20. The linear prediction coefficients of $G^{-1}(q)$ are computed by using the autocorrelation method. The input of the autocorrelation method is clean speech which is constructed by concatenating 26 sentences spoken by 4 different speakers from the TIMIT database [37]. P synthesized SSN signals are produced by using P random WGN sequences as the input of the all-pole filter $G^{-1}(q)$. For each compared AFC method, we run simulation P times for P different synthesized SSN signals. Then we compute the mean misalignments for MIS (Mean MIS) and for MIS_H (Mean MIS_H), respectively, i.e.,

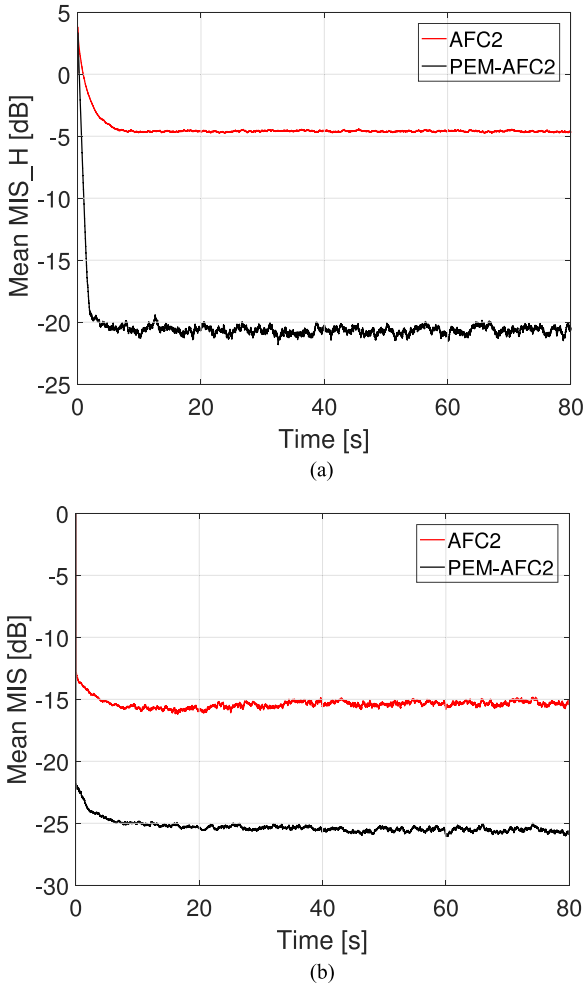

Fig. 6. Performance of the AFC2 and PEM-AFC2 with normal feedback paths for undermodeling case ($\xi(k) \neq 0$), SSNs are incoming signals, a) mean of MIS_H for 10 generated SSNs, b) mean of MIS for 10 generated SSNs.

$$\text{Mean MIS} = \frac{1}{\mathrm{P}}\sum_{i=1}^{\mathrm{P}}\mathrm{MIS}_i, \tag{67}$$

$$\text{Mean MIS\_H} = \frac{1}{\mathrm{P}}\sum_{i=1}^{\mathrm{P}}\left(\mathrm{MIS\_H}\right)_i, \tag{68}$$

where P is the number of simulation times, MIS_i and $\left(\mathrm{MIS\_H}\right)_i$ are the normalized misalignments for estimating $F_1(q)$ and for estimating $H(q)$ with the ith SSN as the incoming signal, respectively. MIS_i and $\left(\mathrm{MIS\_H}\right)_i$ are calculated in a similar way to (64) and (65), respectively. Here $\mathrm{P} = 10$ and the normal feedback paths are selected. In this scenario, the actual $H(q)$ is a random white Gaussian sequence with full length of 20 and a standard deviation of 0.01. Ten random $H(q)$ are generated corresponding to 10 synthesized SSN signals. For the PEM-AFC2 the pre-filter $\hat{G}(q)$ is chosen such that $\hat{G}(q) = G(q)$.

Fig. 6 depicts the performance of the AFC2 method and the PEM-AFC2 for the case of undermodeling the RTF ($\xi(k) \neq 0$).

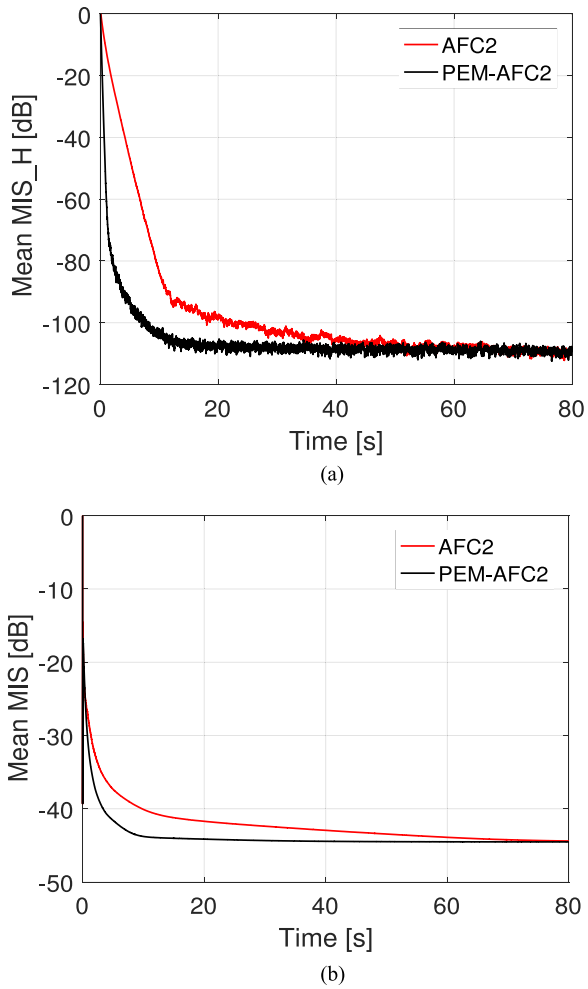

Fig. 7. Performance of the AFC2 and PEM-AFC2 with normal feedback paths for perfect modeling ($\xi(k) = 0$), SSNs are incoming signals, a) mean of MIS_H for 10 generated SSNs, b) mean of MIS for 10 generated SSNs.

The same step-sizes $\mu = 0.001$ are selected for both methods. We can see that the PEM-AFC2 has much lower Mean MIS and Mean MIS_H corresponding to significantly lower bias in both estimates of $F_1(q)$ and $H(q)$ compared to the AFC2. In fact, the PEM-AFC2 provides more than 15 dB lower Mean MIS_H and approximately 10 dB lower Mean MIS. Moreover, the PEM-AFC2 converges faster than the AFC2 method.

Fig. 7 illustrates the performance of the AFC2 method and the PEM-AFC2 for the case of perfect modeling the RTF ($\xi(k) = 0$). To increase convergence rate we choose step-size $\mu = 0.005$ for both methods. Both the AFC2 and the proposed method yield a similar level of Mean MIS_H which reaches to -110 dB when the system converges. This result is consistent with the theoretical analyses in (60), which proves that there is no bias in the estimate of $H(q)$. Fig. 7(b) shows that both mentioned methods reach to the same level of Mean MIS when the system converges. This result is also consistent with the theoretical analyses in (61) which show that both methods obtain the same bias for the estimate of $F_1(q)$. The Mean MIS for both methods can reach up to -45 dB, which is much higher than Mean MIS_H. The reason is that the bias in the estimate of $F_1(q)$ is now decided by the term $\mathbf{f}_{2_h}$.

In the following scenario 2 and scenario 3, we evaluate the performance of the PEM-AFC2 in comparison with the PEM-AFC and the AFC2 for real speech sequences as the incoming signals. The incoming signals are recorded using two microphones which are designed as in [31]. The speech sources are constructed by using 30 IEEE sentences spoken by 3 male and 3 female speakers from NOIZEUS database [38]. In particular, the concatenated speech signal is generated by concatenating all 30 IEEE sentences together. The male speech signal and the female speech signal are produced by concatenating 15 male speech sentences and 15 female sentences, respectively. To obtain the incoming signals of 80 s length the male speech signal and the female speech signal are repeated several times and then truncated after 80 s. We select the step-sizes for all AFC methods such that they provide a similar initial convergence rate. For example, the step size $\mu = 0.001$ is selected for the AFC2 method, whereas $\mu = 0.0005$ is used for both the PEM-AFC and the PEM-AFC2. In all AFC methods using the PEM, a 20-order AR model of the incoming signal is computed for every frame of 160 samples by using the Levinson-Durbin algorithm [39]. To evaluate the quality of the speech signal the perceptual evaluation of speech quality (PESQ) [38] is used. For the PESQ measures, we choose the incoming signal $u_1(k)$ as the reference and the error signal $e_1(k)$ as the test signal. The average misalignment ($\overline{MIS}$) and average added stable gain ($\overline{ASG}$) are also computed over whole 80 s (i.e., 1280000 samples) of each realization.

Scenario 2: in this scenario, the feedback paths are normal feedback paths and the incoming signals are concatenated speech.

Fig. 8 depicts the performance of all considered AFC methods for the second scenario. It can be seen that the AFC2 method outperforms the PEM-AFC and the PEM-AFC2 outperforms the AFC2 method. The variation of the normalized MIS and ASG values over time in case of the PEM-AFC may come from the model mismatch between $G(q)$ and $\hat{G}(q)$, whereas in the AFC2 method it may come from the model mismatch between the true $H(q)$ and the estimated $\hat{H}(q)$. That variation in the PEM-AFC2 method may be caused by both above reasons.

Table I shows that all considered AFC methods achieve high perceptual speech quality. The PESQ scores of the AFC2 and the PEM-AFC2 are similar but higher than that of the PEM-AFC. Moreover, the proposed PEM-AFC2 provides much better average misalignment ($\overline{MIS}$) and average added stable gain ($\overline{ASG}$), for instance, approximately 6.4 dB $\overline{MIS}$ gain and 7.3 dB $\overline{ASG}$ gain compared to the PEM-AFC, 2.6 dB $\overline{MIS}$ gain and 2.3 dB $\overline{ASG}$ gain compared to the AFC2 method.

We also measure the PESQ of the HA without using control algorithm, $PESQ = 3.61$. It demonstrates that the PEM-AFC, the AFC2 method and the PEM-AFC2 provide an improvement of 0.82, 0.87 and 0.86 scores in PESQ compared to the case without control algorithm, respectively. The comparable PESQ scores among three considered AFC methods are expected due to the fact that the maximum stable gain of the system without

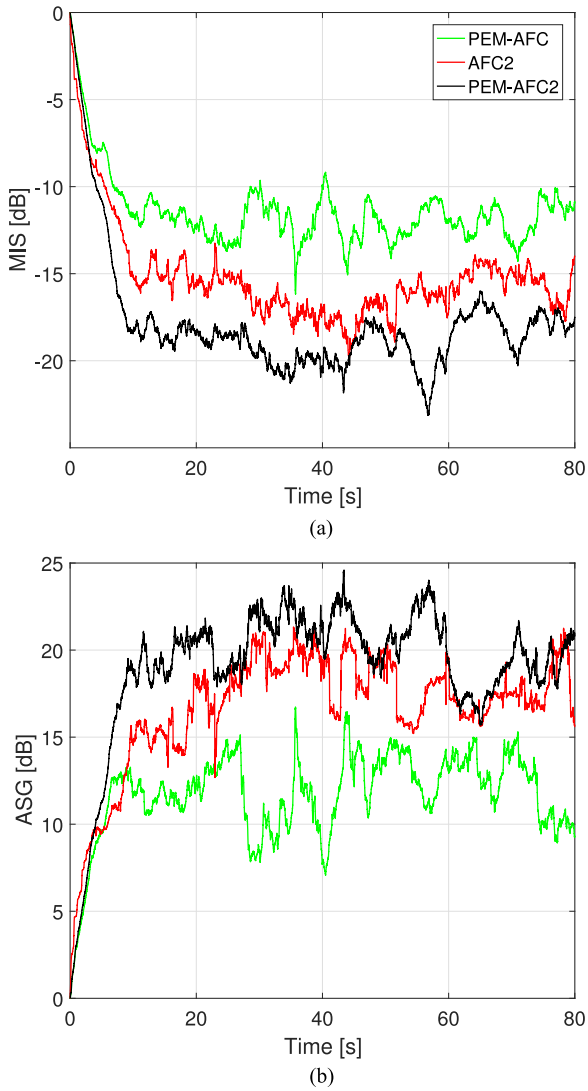

Fig. 8. Performance of the PEM-AFC, AFC2 and PEM-AFC2 with normal feedback paths, concatenated speech incoming signals. (a) Misalignment. (b) Added Stable Gain.

feedback cancellation is approximately 27–29 dB (the maximum of F1 in Fig. 5). With the applied forward path gain of 30 dB, the system is approximately 3 dB overcritical. Hence, once the ASG is larger than approximately 5–6 dB, there will be almost no audible artifacts. Since all considered AFC methods reach this point of 5–6 dB ASG after a very similar time period (approximately 2–3 s) and only this period will contribute distortions that may make a difference in the PESQ scores, the PESQ scores are quite similar among those methods.

To statistically evaluate the differences in the PESQ among compared AFC methods, we repeat the same experiment for 9 different incoming signals which are produced by concatenating 30 IEEE speech sentences extracted from NOIZEUS database with different order. We use a one-way analysis of variance (ANOVA) to calculate the mean value and the 95 percent confidence interval (CI) over ten above PESQ measures (including the first measure as shown in Table I) for each AFC method. The results are $\{3.616, [3.609, 3.622]\}$, $\{4.418, [4.412, 4.425]\}$, $\{4.481, [4.474, 4.487]\}$ and $\{4.458, [4.451, 4.464]\}$ for the HA

TABLE I
EVALUATE PERFORMANCE OF PEM-AFC, AFC2, PEM-AFC2 FOR CONCATENATED SPEECH INCOMING SIGNALS, NORMAL FEEDBACK PATHS

AFC methods	$PESQ$	$\overline{MIS}$	$\overline{ASG}$
PEM-AFC	4.43	−11.42	11.69
AFC2	4.48	−15.23	16.67
PEM-AFC2	4.47	−17.86	19.03

without using control algorithm, the PEM-AFC, the AFC2 method, and the PEM-AFC2, respectively, where the first term in the parenthesis indicates the mean value and the second term (bounded by square brackets) indicates the lower and upper limits for 95 percent CIs for the mean. It can be seen that the 95 percent CIs of all mentioned AFC methods are not overlapped. Hence, the mean PESQ is significantly different across measures using those AFC methods. To determine which AFC methods make a difference in the PESQ, we perform a multiple comparison test using the Bonferroni method. The test shows that all obtained p-values are smaller than 0.05, i.e., the mean PESQ measures of all mentioned AFC methods significantly differ across all AFC methods.

Scenario 3: in the third scenario, the feedback paths have been changed from the normal to the closest feedback paths in the middle of simulation time. The performance of the proposed method is evaluated for three types of incoming signals, including concatenated speech, male speech and female speech.

From Figs. 9–11 we observe that the proposed PEM-AFC2 outperforms the PEM-AFC, even when the feedback paths suddenly change after 40 s. It also outperforms the AFC2 method for the normal feedback paths as well as provides lower misalignment and higher added stable gain for the closest feedback paths. Especially, the PEM-AFC2 can track the change of the channels much quicker than both the PEM-AFC and the AFC2 method. In particular, in the first 2 seconds after the change of the feedback paths, the proposed method achieves approximately 3 dB improvement in normalized misalignment compared to the two remaining methods when the incoming signals are male speech. For both cases that concatenated speech and female speech are used as the incoming signals, those improvements are approximately 5 dB and 3 dB, respectively, compared to the PEM-AFC and the AFC2 method.

We recognize that both the AFC2 and PEM-AFC2 obtain less improvement on MIS and ASG for the closest feedback paths than for the normal feedback paths because now the second feedback paths (corresponding to the closest feedback paths) are strong, i.e., the value of term $\mathbf{f}_{2_h}$ is large, leading to a large bias in the estimation of the feedback path. These results match well with the theoretical analysis.

Table II summarizes the experimental results of PESQ, average MIS and average ASG for all considered AFC methods. The $\overline{MIS}1$ and $\overline{ASG}1$ present the average MIS and average ASG before the feedback paths change, whereas the $\overline{MIS}2$ and $\overline{ASG}2$ are those values after the change. All methods have PESQ scores larger than 4.4. However, the PEM-AFC2 obtains about 5.6–6.5 dB $\overline{MIS}$ 1 gain and 5.6–8.0 dB $\overline{ASG}$ 1 gain compared to the PEM-AFC as well as approximately 2.7 dB $\overline{MIS}$ 1 gain

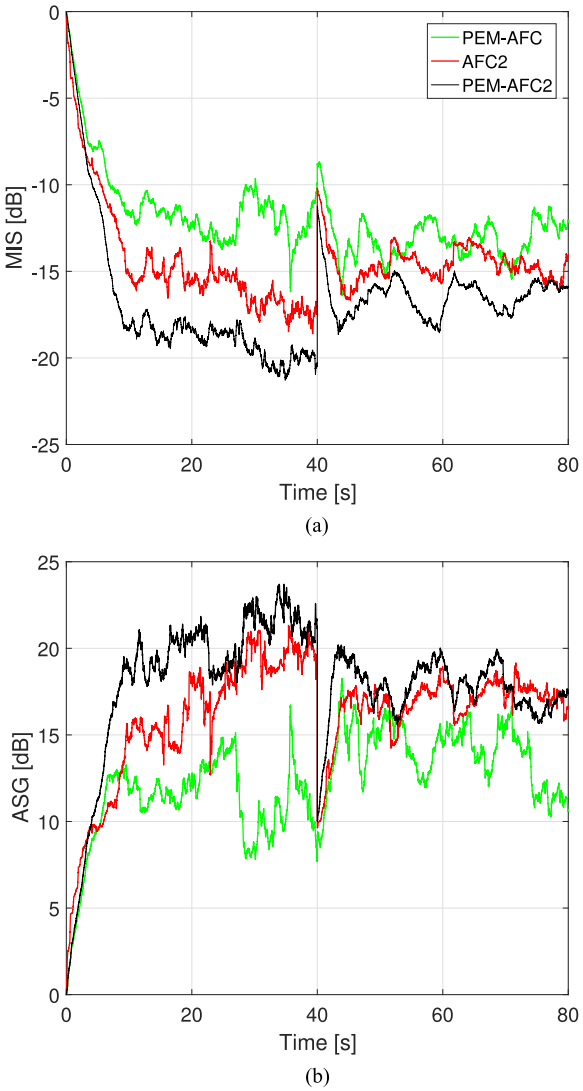

Fig. 9. Performance of the PEM-AFC, AFC2 and PEM-AFC2 with a sudden change of feedback paths from normal to closest feedback paths after 40 s, concatenated speech incoming signal. (a) Misalignment. (b) Added Stable Gain.

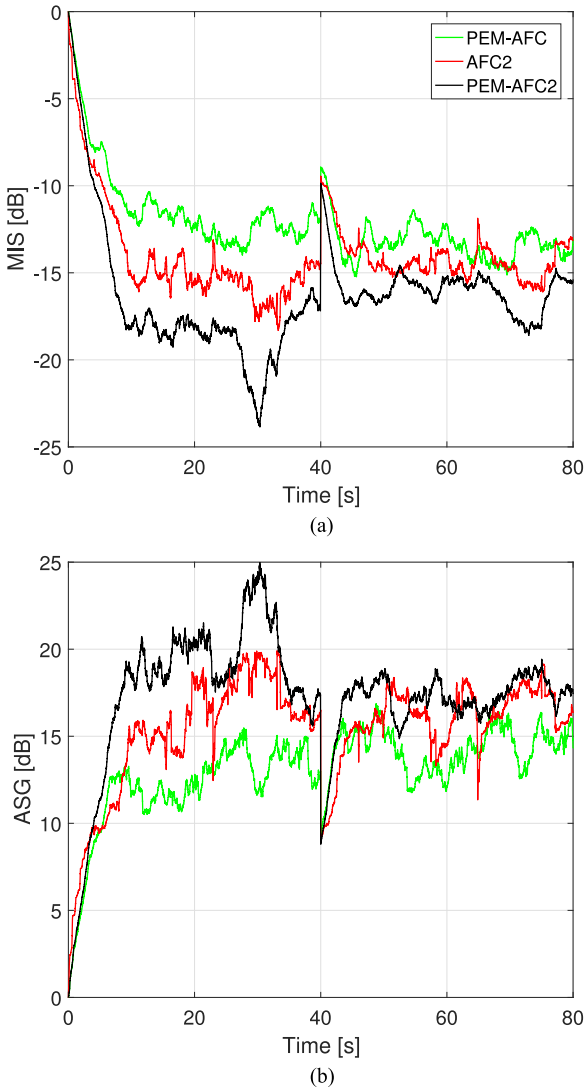

Fig. 10. Performance of the PEM-AFC, AFC2 and PEM-AFC2 with a sudden change of feedback paths from normal to closest feedback paths after 40 s, male speech incoming signal. (a) Misalignment. (b) Added Stable Gain.

and 2.5–3.8 dB $\overline{ASG}$ 1 gain compared to the AFC2 method. After the feedback paths change, the PEM-AFC2 achieves approximately 2.7–3.8 dB $\overline{MIS}$ 2 gain and 2.8–5.0 dB $\overline{ASG}$ 2 gain compared to the PEM-AFC as well as approximately 2 dB $\overline{MIS}$ 2 gain and 1 dB $\overline{ASG}$ 2 gain compared to the AFC2 method.

Scenario 4: in this scenario, we evaluate the proposed PEM-AFC2 with music as the incoming signal and with a sudden change of the feedback paths after 40 s. The song "Imagine" by John Lennon is selected as the music signal. The same setup that is used in the scenario 3 is chosen, except a 51-order AR model of the incoming signal is selected. Since the music incoming signal is harder to be modeled than the speech incoming signal [40], a higher order is selected for the AR model in order to improve the modeling accuracy, resulting in an improved system performance. Furthermore, we utilize the perceptual evaluation of audio quality (PEAQ) measure [41] to evaluate the quality of the music signal. For the PEAQ measures, we also choose the incoming signal $u_1(k)$ as the reference and the error signal $e_1(k)$ as the test signal.

Fig. 12 demonstrates the performance of the proposed method in comparison with the PEM and the AFC2 method for this scenario. It can be seen that the PEM-AFC2 outperforms the two other mentioned methods not only before the feedback paths change, but also after the change. Although the proposed method yields large variations after a sudden change of the feedback paths due to the larger mismatch in modeling the music incoming signal in this situation, it still provides lower misalignment, higher ASG, and quicker tracking rate than the PEM and the AFC2 method.

Table III compares the average MIS and the average ASG of three mentioned AFC methods before and after the feedback paths change. It shows that the proposed PEM-AFC2 achieves approximately 7 dB gain compared to two remaining AFC methods before the change and 5 dB gain compared to the PEM-AFC, 2 dB gain compared to the AFC2 method after the change.

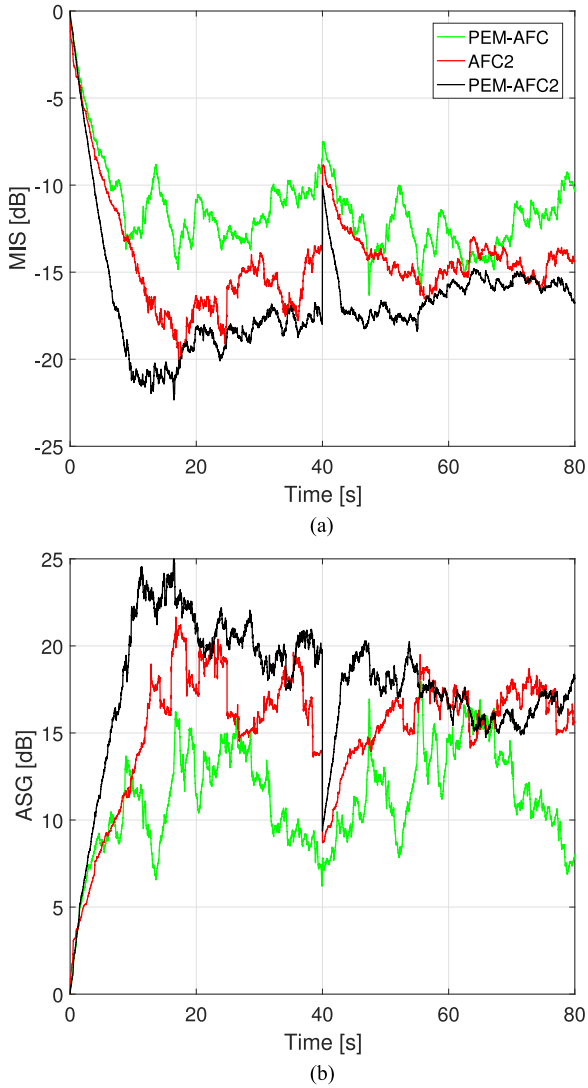

Fig. 11. Performance of the PEM-AFC, AFC2 and PEM-AFC2 with a sudden change of feedback paths from normal to closest feedback paths after 40 s, female speech incoming signal. (a) Misalignment. (b) Added Stable Gain.

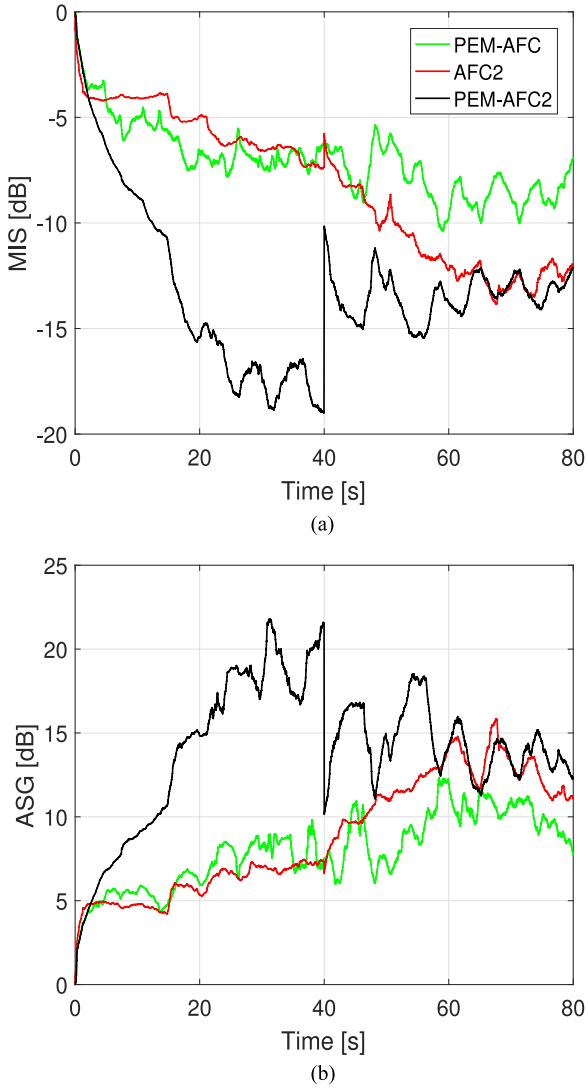

Fig. 12. Performance of the PEM-AFC, AFC2 and PEM-AFC2 with a sudden change of feedback paths from normal to closest feedback paths after 40 s, music as the incoming signal. (a) Misalignment. (b) Added Stable Gain.

TABLE II
EVALUATE PERFORMANCE OF PEM-AFC, AFC2, PEM-AFC2 FOR DIFFERENT TYPES OF SPEECH AS THE INCOMING SIGNALS, FEEDBACK PATHS CHANGE FROM NORMAL TO CLOSEST FEEDBACK PATHS AFTER 40 S

AFC methods	Incoming signals	PESQ	$\overline{MIS}1$	$\overline{ASG}1$	$\overline{MIS}2$	$\overline{ASG}2$
PEM-AFC	Male speech	4.45	−11.05	11.86	−13.23	14.23
AFC2		4.48	−13.95	14.91	−14.16	15.92
PEM-AFC2		4.47	−16.69	17.51	−15.95	17.01
PEM-AFC	Female speech	4.39	−10.69	10.62	−12.31	11.91
AFC2		4.47	−14.47	14.79	−14.18	15.73
PEM-AFC2		4.46	−17.21	18.59	−16.14	16.87
PEM-AFC	Concatenated speech	4.43	−10.86	10.87	−13.07	13.90
AFC2		4.48	−14.28	15.60	−14.56	16.72
PEM-AFC2		4.47	−17.00	18.11	−16.43	17.65

TABLE III
EVALUATE AVERAGE MIS AND AVERAGE ASG OF PEM-AFC, AFC2, PEM-AFC2 FOR MUSIC AS THE INCOMING SIGNAL, FEEDBACK PATHS CHANGE FROM NORMAL TO CLOSEST FEEDBACK PATHS AFTER 40 S

AFC methods	$\overline{MIS}1$	$\overline{ASG}1$	$\overline{MIS}2$	$\overline{ASG}2$
PEM-AFC	−5.99	6.54	−8.10	9.45
AFC2	−5.30	5.82	−11.16	11.95
PEM-AFC2	−13.05	13.73	−13.43	14.35

Table IV evaluates the signal quality of those AFC methods using PEAQ measures. It shows that three AFC methods have the same PEAQ scores for the initial convergence phase (0 s–5 s). The reason is that the step-sizes are selected such that all the AFC methods have the same initial convergence. However, for the first convergence phase (30 s–35 s), i.e., before the change of the feedback paths, the proposed method obtains the PEAQ score of −0.59 corresponding to a very good signal quality (almost imperceptible), whereas the PEM-AFC and the AFC2

TABLE IV
EVALUATE PEAQ MEASURES OF PEM-AFC, AFC2, PEM-AFC2 FOR MUSIC AS THE INCOMING SIGNAL, FEEDBACK PATHS CHANGE FROM NORMAL TO CLOSEST FEEDBACK PATHS AFTER 40 S

AFC methods	PEAQ (0 s–5 s)	PEAQ (30 s–35 s)	PEAQ (38 s–43 s)	PEAQ (70 s–75 s)
PEM-AFC	−2.20	−2.18	−2.11	−2.17
AFC2	−2.20	−2.20	−2.20	−1.61
PEM-AFC2	−2.20	−0.59	−0.10	−0.14

TABLE V
COMPUTATIONAL COMPLEXITY PER OUTPUT SAMPLE

AFC methods	Computational complexity	#
PEM-AFC	$\frac{5P_0^2+2LP_0+P_0}{2L} + 2P_0 + 3L_{\hat{f}} + 2$	134
AFC2	$3\left(L_{\hat{f}} + L_{\hat{h}}\right) + 4$	100
PEM-AFC2	$\frac{5P_0^2+2LP_0+P_0}{2L} + 3P_0 + 3\left(L_{\hat{f}} + L_{\hat{h}}\right) + 4$	186

A numerical value is given for $P_0 = 20$, $L = 160$, $L_{\hat{f}} = 22$, and $L_{\hat{h}} = 10$.

method get the PEAQ score approximately -2 corresponding to a moderate signal quality (slightly annoying). Similar results are achieved for the re-convergence phase (38 s–43 s). During the second convergence phase (70 s–75 s), i.e., after the change of the feedback paths, the PEAQ score of the AFC2 method and the PEM are -1.61 (between perceptible but not annoying and slightly annoying), and -2.17 (slightly annoying), respectively. However, the PEAQ score of the proposed method in this case is -0.1 (almost imperceptible). Overall, the proposed method provides better signal quality than two remaining methods for music incoming signal.

VII. COMPUTATIONAL COMPLEXITY

In this section, we provide a computational complexity comparison among the proposed PEM-AFC2, the PEM-AFC and the AFC2 methods. Table V summarizes the number of real multiplications per output sample [42] for the three considered AFC methods, where we assume that a real mutiplication and a real division have equal complexity. Generally, the proposed method has a larger computational complexity than either the PEM-AFC or the AFC2 method. In the PEM-AFC2 method $\hat{H}(q)$ as well as the LPC coefficients need to be estimated, whereas in the AFC2 method only the $\hat{H}(q)$ needs to be estimated and in the PEM-AFC method only the LPC coefficients need to be estimated. In particular, the computational complexity for estimating the LPC coefficients using the autocorrelation matrix and the Levinson-Durbin algorithm is $\frac{5P_0^2+2LP_0+P_0}{2L}$ mutiplications, where P_0 is the AR-model order and L is the frame length. In addition, the pre-whitened signal at the output of each pre-filter is computed using P_0 mutiplications. The complexity for estimating the adaptive filter coefficients using NLMS algorithm is $3n + 2$ mutiplications, where n is the adaptive filter order [43].

VIII. CONCLUSION

In this paper, a new derivation for optimal filters in the AFC2 method, which provides an actual optimal solution to the problem stated in [31], has been developed. Moreover, to further reduce the bias we have proposed the PEM-AFC2 which used pre-filters to pre-whiten the input signals of adaptive filters for the adaptive feedback control in the two-microphone hearing aids. The PEM-AFC2 has been theoretically analyzed and we found that an improved solution for the identifications of the feedback path $F_1(q)$ as well as the RTF $H(q)$ compared to the PEM-AFC and the AFC2 method was obtained when the PEM has been applied for the AFC2 method. The experimental results with correct assumptions match perfectly with the theoretical analyses for both undermodeling the RTF as well as perfect modeling the RTF. Furthermore, the experimental results also show that the proposed PEM-AFC2 yields a significant performance improvement in terms of MIS and ASG compared to other state-of-the-art methods such as the PEM-AFC or the AFC2 for music and different types of speech incoming signals as well as with a sudden change of the feedback paths. It also obtains as good signal quality as the two compared methods for speech incoming signals, but better signal quality for music incoming signals. In addition, the PEM-AFC2 converges faster and can track the sudden change of the feedback paths quicker than the PEM-AFC as well as the AFC2 method.

APPENDIX A
FIRST APPENDIX

The following derivations show how to compute the terms $\boldsymbol{R}_{\mathbf{z}_1}^{-1}\boldsymbol{R}_{\mathbf{z}_1\mathbf{z}_2}\mathbf{b}$ and $\boldsymbol{R}_{\mathbf{z}_1}^{-1}\boldsymbol{r}_{\mathbf{z}_1\xi}$ in subsection IV-C.

Firstly, the auto-correlation matrix $\boldsymbol{R}_{\mathbf{z}_1}$ and the cross-correlation matrix $\boldsymbol{R}_{\mathbf{z}_1\mathbf{z}_2}$ can be computed as

$$\boldsymbol{R}_{\mathbf{z}_1} = \begin{bmatrix} \boldsymbol{R}_{\mathbf{y}} & \boldsymbol{R}_{\mathbf{y}\mathbf{x}_2} \\ \boldsymbol{R}_{\mathbf{x}_2\mathbf{y}} & \boldsymbol{R}_{\mathbf{x}_2} \end{bmatrix} \tag{A.1}$$

and

$$\boldsymbol{R}_{\mathbf{z}_1\mathbf{z}_2} = \begin{bmatrix} \boldsymbol{R}_{\mathbf{y}} & \boldsymbol{R}_{\mathbf{y}\mathbf{u}_2} \\ \boldsymbol{R}_{\mathbf{x}_2\mathbf{y}} & \boldsymbol{R}_{\mathbf{x}_2\mathbf{u}_2} \end{bmatrix}. \tag{A.2}$$

Hence,

$$\boldsymbol{R}_{\mathbf{z}_1}^{-1} = \begin{bmatrix} \boldsymbol{M} & \boldsymbol{N} \\ \boldsymbol{N}^T & \boldsymbol{Q} \end{bmatrix} \tag{A.3}$$

where $\boldsymbol{Q} = \left(\boldsymbol{R}_{\mathbf{x}_2} - \boldsymbol{R}_{\mathbf{x}_2\mathbf{y}}\boldsymbol{R}_{\mathbf{y}}^{-1}\boldsymbol{R}_{\mathbf{y}\mathbf{x}_2}\right)^{-1}$, $\boldsymbol{N} = -\boldsymbol{R}_{\mathbf{y}}^{-1}\boldsymbol{R}_{\mathbf{y}\mathbf{x}_2}\left(\boldsymbol{R}_{\mathbf{x}_2} - \boldsymbol{R}_{\mathbf{x}_2\mathbf{y}}\boldsymbol{R}_{\mathbf{y}}^{-1}\boldsymbol{R}_{\mathbf{y}\mathbf{x}_2}\right)^{-1} = -\boldsymbol{R}_{\mathbf{y}}^{-1}\boldsymbol{R}_{\mathbf{y}\mathbf{x}_2}\boldsymbol{Q}$ and $\boldsymbol{M} = \boldsymbol{R}_{\mathbf{y}}^{-1} - \boldsymbol{N}\boldsymbol{R}_{\mathbf{x}_2\mathbf{y}}\boldsymbol{R}_{\mathbf{y}}^{-1}$.

Then, we compute

$$\begin{aligned} \boldsymbol{R}_{\mathbf{z}_1\mathbf{z}_2}\mathbf{b} &= \begin{bmatrix} \boldsymbol{R}_{\mathbf{y}} & \boldsymbol{R}_{\mathbf{y}\mathbf{u}_2} \\ \boldsymbol{R}_{\mathbf{x}_2\mathbf{y}} & \boldsymbol{R}_{\mathbf{x}_2\mathbf{u}_2} \end{bmatrix} \begin{bmatrix} \mathbf{f}_1 \\ \mathbf{h} \end{bmatrix} \\ &= \begin{bmatrix} \boldsymbol{R}_{\mathbf{y}}\mathbf{f}_1 + \boldsymbol{R}_{\mathbf{y}\mathbf{u}_2}\mathbf{h} \\ \boldsymbol{R}_{\mathbf{x}_2\mathbf{y}}\mathbf{f}_1 + \boldsymbol{R}_{\mathbf{x}_2\mathbf{u}_2}\mathbf{h} \end{bmatrix}. \end{aligned} \tag{A.4}$$

Let $\boldsymbol{X} = \boldsymbol{R}_{\mathbf{y}}\mathbf{f}_1 + \boldsymbol{R}_{\mathbf{y}\mathbf{u}_2}\mathbf{h}$ and $\boldsymbol{Y} = \boldsymbol{R}_{\mathbf{x}_2\mathbf{y}}\mathbf{f}_1 + \boldsymbol{R}_{\mathbf{x}_2\mathbf{u}_2}\mathbf{h}$, we obtain

$$\boldsymbol{R}_{\mathbf{z}_1}^{-1}\boldsymbol{R}_{\mathbf{z}_1\mathbf{z}_2}\mathbf{b} = \begin{bmatrix} \boldsymbol{M} & \boldsymbol{N} \\ \boldsymbol{N}^T & \boldsymbol{Q} \end{bmatrix} \begin{bmatrix} \boldsymbol{X} \\ \boldsymbol{Y} \end{bmatrix} = \begin{bmatrix} \boldsymbol{M}\boldsymbol{X} + \boldsymbol{N}\boldsymbol{Y} \\ \boldsymbol{N}^T\boldsymbol{X} + \boldsymbol{Q}\boldsymbol{Y} \end{bmatrix}. \quad \text{(A.5)}$$

However,

$$\boldsymbol{M}\boldsymbol{X} + \boldsymbol{N}\boldsymbol{Y} = \mathbf{f}_1 + \boldsymbol{R}_{\mathbf{y}}^{-1}\boldsymbol{R}_{\mathbf{y}\mathbf{u}_2}\mathbf{h} - \boldsymbol{N}\boldsymbol{R}_{\mathbf{x}_2\mathbf{y}}\boldsymbol{R}_{\mathbf{y}}^{-1}\boldsymbol{R}_{\mathbf{y}\mathbf{u}_2}\mathbf{h} + \boldsymbol{N}\boldsymbol{R}_{\mathbf{x}_2\mathbf{u}_2}\mathbf{h}, \quad \text{(A.6)}$$

and

$$\boldsymbol{N}^T\boldsymbol{X} + \boldsymbol{Q}\boldsymbol{Y} = \boldsymbol{Q}\left(\boldsymbol{R}_{\mathbf{x}_2\mathbf{u}_2}\mathbf{h} - \boldsymbol{R}_{\mathbf{x}_2\mathbf{y}}\boldsymbol{R}_{\mathbf{y}}^{-1}\boldsymbol{R}_{\mathbf{y}\mathbf{u}_2}\mathbf{h}\right), \quad \text{(A.7)}$$

due to $\boldsymbol{R}_{\mathbf{y}}^T = \boldsymbol{R}_{\mathbf{y}}$, $\boldsymbol{R}_{\mathbf{x}_2}^T = \boldsymbol{R}_{\mathbf{x}_2}$, $\boldsymbol{Q}^T = \boldsymbol{Q}$.

We reformulate (16) as

$$u_2 = x_2 - F_2(q)\, y, \quad \text{(A.8)}$$

then multiply $H(q)$ with both sides of that equation, i.e.,

$$H(q)\, u_2 = H(q)\, x_2 - H(q)\, F_2(q)\, y,$$

or

$$\mathbf{h}^T\mathbf{u}_2 = \mathbf{h}^T\mathbf{x}_2 - \mathbf{f}_{2_{\mathbf{h}}}^T\mathbf{y}, \quad \text{(A.9)}$$

where $\mathbf{f}_{2_{\mathbf{h}}}$ is a coefficient vector of $H(q)\, F_2(q)$. Computing the expectation of the vector $\mathbf{x}_2$ with each side of (A.9) yields

$$E\left\{\mathbf{x}_2\left[\mathbf{h}^T\mathbf{u}_2\right]^T\right\} = E\left\{\mathbf{x}_2\left[\mathbf{h}^T\mathbf{x}_2(k) - \mathbf{f}_{2_{\mathbf{h}}}^T\mathbf{y}\right]^T\right\},$$

$$\boldsymbol{R}_{\mathbf{x}_2\mathbf{u}_2}\mathbf{h} = \boldsymbol{R}_{\mathbf{x}_2}\mathbf{h} - \boldsymbol{R}_{\mathbf{x}_2\mathbf{y}}\mathbf{f}_{2_{\mathbf{h}}}. \quad \text{(A.10)}$$

Similarly, we obtain

$$E\left\{\mathbf{y}\left[\mathbf{h}^T\mathbf{u}_2\right]^T\right\} = E\left\{\mathbf{y}\left[\mathbf{h}^T\mathbf{x}_2 - \mathbf{f}_{2_{\mathbf{h}}}^T\mathbf{y}\right]^T\right\},$$

$$\boldsymbol{R}_{\mathbf{y}\mathbf{u}_2}\mathbf{h} = \boldsymbol{R}_{\mathbf{y}\mathbf{x}_2}\mathbf{h} - \boldsymbol{R}_{\mathbf{y}}\mathbf{f}_{2_{\mathbf{h}}}. \quad \text{(A.11)}$$

By substituting (A.10) and (A.11) into (A.6) and (A.7), we achieve

$$\boldsymbol{M}\boldsymbol{X} + \boldsymbol{N}\boldsymbol{Y} = \mathbf{f}_1 - \mathbf{f}_{2_{\mathbf{h}}}, \quad \text{(A.12)}$$

$$\boldsymbol{N}^T\boldsymbol{X} + \boldsymbol{Q}\boldsymbol{Y} = \mathbf{h}. \quad \text{(A.13)}$$

Moreover,

$$\boldsymbol{R}_{\mathbf{z}_1}^{-1}\boldsymbol{r}_{\mathbf{z}_1\xi} = \begin{bmatrix} \boldsymbol{M} & \boldsymbol{N} \\ \boldsymbol{N}^T & \boldsymbol{Q} \end{bmatrix} \begin{bmatrix} \boldsymbol{r}_{\mathbf{y}\xi} \\ \boldsymbol{r}_{\mathbf{x}_2\xi} \end{bmatrix} = \begin{bmatrix} \boldsymbol{M}\boldsymbol{r}_{\mathbf{y}\xi} + \boldsymbol{N}\boldsymbol{r}_{\mathbf{x}_2\xi} \\ \boldsymbol{N}^T\boldsymbol{r}_{\mathbf{y}\xi} + \boldsymbol{Q}\boldsymbol{r}_{\mathbf{x}_2\xi} \end{bmatrix} = \begin{bmatrix} \boldsymbol{B}_1 \\ \boldsymbol{B}_{\mathbf{h}} \end{bmatrix}, \quad \text{(A.14)}$$

where

$$\boldsymbol{B}_1 = \boldsymbol{M}\boldsymbol{r}_{\mathbf{y}\xi} + \boldsymbol{N}\boldsymbol{r}_{\mathbf{x}_2\xi}, \quad \text{(A.15)}$$

$$\boldsymbol{B}_{\mathbf{h}} = \boldsymbol{N}^T\boldsymbol{r}_{\mathbf{y}\xi} + \boldsymbol{Q}\boldsymbol{r}_{\mathbf{x}_2\xi}. \quad \text{(A.16)}$$

APPENDIX B
SECOND APPENDIX

This appendix provides proofs for the equality in (56) and (57). Due to the assumption in (43) and if $\hat{G}(q) = G(q)$, we obtain $u_{2p}(k) = \hat{G}(q)\, G^{-1}(q)\, w(k) = w(k)$. Thus the cross-correlation between the whitened loudspeaker signal vector $\mathbf{y}_p(k)$ and the whitened second incoming signal vector $\mathbf{u}_{2p}(k) = \mathbf{w}(k)$ is zero if the condition $d_k > L_{\hat{h}} - 1$ is fulfilled, i.e.,

$$\boldsymbol{R}_{\mathbf{y}_p\mathbf{u}_{2p}} = E\left\{\mathbf{y}_p(k)\,\mathbf{u}_{2p}^T(k)\right\} = E\left\{\mathbf{y}_p(k)\,\mathbf{w}^T(k)\right\} = \mathbf{0}. \quad \text{(B.1)}$$

Moreover, from (16) and (46), we obtain $x_{2p}(k) = w(k) + F_2(q)\, y_p(k)$. Hence,

$$\boldsymbol{R}_{\mathbf{x}_{2p}\mathbf{u}_{2p}} = E\left\{\mathbf{x}_{2p}(k)\,\mathbf{u}_{2p}^T(k)\right\} = E\left\{\mathbf{x}_{2p}(k)\,\mathbf{w}^T(k)\right\} = \boldsymbol{R}_{\mathbf{w}}. \quad \text{(B.2)}$$

By using the pre-filter $\hat{G}(q)$ in the PEM-AFC2 model, the (A.10), (A.11) in Appendix A can be reformulated as follows

$$\boldsymbol{R}_{\mathbf{w}}\mathbf{h} = \boldsymbol{R}_{\mathbf{x}_{2p}}\mathbf{h} - \boldsymbol{R}_{\mathbf{x}_{2p}\mathbf{y}_p}\mathbf{f}_{2_{\mathbf{h}}}, \quad \text{(B.3)}$$

$$\boldsymbol{R}_{\mathbf{y}_p\mathbf{u}_{2p}}\mathbf{h} = \boldsymbol{R}_{\mathbf{y}_p\mathbf{x}_{2p}}\mathbf{h} - \boldsymbol{R}_{\mathbf{y}_p}\mathbf{f}_{2_{\mathbf{h}}}. \quad \text{(B.4)}$$

By substituting (B.1) and (B.2) into (B.3) and (B.4), we obtain

$$\left(\boldsymbol{R}_{\mathbf{x}_{2p}} - \boldsymbol{R}_{\mathbf{w}}\right)\mathbf{h} = \boldsymbol{R}_{\mathbf{x}_{2p}\mathbf{y}_p}\mathbf{f}_{2_{\mathbf{h}}},$$

$$\boldsymbol{R}_{\mathbf{y}_p\mathbf{x}_{2p}}\mathbf{h} = \boldsymbol{R}_{\mathbf{y}_p}\mathbf{f}_{2_{\mathbf{h}}}.$$

Hence,

$$\mathbf{h} = \left(\boldsymbol{R}_{\mathbf{x}_{2p}} - \boldsymbol{R}_{\mathbf{w}}\right)^{-1}\boldsymbol{R}_{\mathbf{x}_{2p}\mathbf{y}_p}\mathbf{f}_{2_{\mathbf{h}}}, \quad \text{(B.5)}$$

$$\mathbf{f}_{2_{\mathbf{h}}} = \boldsymbol{R}_{\mathbf{y}_p}^{-1}\boldsymbol{R}_{\mathbf{y}_p\mathbf{x}_{2p}}\mathbf{h}. \quad \text{(B.6)}$$

Moreover, substituting (B.6) into (B.5) yields

$$\mathbf{h} = \left(\boldsymbol{R}_{\mathbf{x}_{2p}} - \boldsymbol{R}_{\mathbf{w}}\right)^{-1}\boldsymbol{R}_{\mathbf{x}_{2p}\mathbf{y}_p}\boldsymbol{R}_{\mathbf{y}_p}^{-1}\boldsymbol{R}_{\mathbf{y}_p\mathbf{x}_{2p}}\mathbf{h},$$

leading to

$$\left(\boldsymbol{R}_{\mathbf{x}_{2p}} - \boldsymbol{R}_{\mathbf{w}}\right)^{-1}\boldsymbol{R}_{\mathbf{x}_{2p}\mathbf{y}_p}\boldsymbol{R}_{\mathbf{y}_p}^{-1}\boldsymbol{R}_{\mathbf{y}_p\mathbf{x}_{2p}} = \mathbf{I},$$

where $\mathbf{I}$ is the $(L_h \times L_h)$ identity matrix.

As a result,

$$\boldsymbol{R}_{\mathbf{x}_{2p}} - \boldsymbol{R}_{\mathbf{w}} = \boldsymbol{R}_{\mathbf{x}_{2p}\mathbf{y}_p}\boldsymbol{R}_{\mathbf{y}_p}^{-1}\boldsymbol{R}_{\mathbf{y}_p\mathbf{x}_{2p}}. \quad \text{(B.7)}$$

Furthermore, we also have $\boldsymbol{R}_{\mathbf{y}_p}^T = \boldsymbol{R}_{\mathbf{y}_p}$, $\boldsymbol{R}_{\mathbf{x}_{2p}}^T = \boldsymbol{R}_{\mathbf{x}_{2p}}$, $\tilde{\boldsymbol{Q}}^T = \tilde{\boldsymbol{Q}}$.

From the (B.7) and the definitions of $\tilde{\boldsymbol{Q}}$ and $\tilde{\boldsymbol{N}}$ in Section V we obtain

$$\tilde{\boldsymbol{Q}} = \boldsymbol{R}_{\mathbf{w}}^{-1}, \quad \text{(B.8)}$$

$$\tilde{\boldsymbol{N}} = -\boldsymbol{R}_{\mathbf{y}_p}^{-1}\boldsymbol{R}_{\mathbf{y}_p\mathbf{x}_{2p}}\boldsymbol{R}_{\mathbf{w}}^{-1} \quad \text{(B.9)}$$

.

If the RTF is undermodeled ($\xi(k) \neq 0$), we rewrite $\xi_p(k)$ as follows

$$\begin{aligned}\xi_p(k) &= \mathbf{h}_{\text{res}}^T \mathbf{u}_{2p}(k) \\ &= \mathbf{h}_{\text{res}}^T \mathbf{w}(k). \end{aligned} \tag{B.10}$$

The cross-correlations $\boldsymbol{r}_{\mathbf{y}_p \xi_p}$ and $\boldsymbol{r}_{\mathbf{x}_{2p} \xi_p}$ are calculated as

$$\boldsymbol{r}_{\mathbf{y}_p \xi_p} = \boldsymbol{R}_{\mathbf{y}_p \mathbf{w}} \mathbf{h}_{\text{res}} = \mathbf{0}, \tag{B.11}$$

$$\boldsymbol{r}_{\mathbf{x}_{2p} \xi_p} = \boldsymbol{r}_{\mathbf{w} \xi_p} = \boldsymbol{R}_{\mathbf{w}} \mathbf{h}_{\text{res}}, \tag{B.12}$$

due to $\boldsymbol{R}_{\mathbf{y}_p \mathbf{w}} = \mathbf{0}$ if $d_k > L_{h_{\text{full}}} - 1$. By substituting (B.11), (B.12) and (B.8), (B.9) into (54) and (55) we achieve

$$\tilde{\boldsymbol{B}}_{\mathbf{h}} = \mathbf{h}_{\text{res}}, \tag{B.13}$$

$$\tilde{\boldsymbol{B}}_1 = -\boldsymbol{R}_{\mathbf{y}_p}^{-1} \boldsymbol{R}_{\mathbf{y}_p \mathbf{x}_{2p}} \mathbf{h}_{\text{res}}. \tag{B.14}$$

For perfect modeling case, $\xi(k) = 0$, i.e., $\mathbf{h}_{\text{res}} = \mathbf{0}$, we obtain

$$\tilde{\boldsymbol{B}}_{\mathbf{h}} = \mathbf{0}, \tag{B.15}$$

$$\tilde{\boldsymbol{B}}_1 = \mathbf{0}. \tag{B.16}$$

REFERENCES

[1] M. G. Siqueira and A. Alwan, "Steady-state analysis of continuous adaptation in acoustic feedback reduction systems for hearing-aids," *IEEE Trans. Speech Audio Process.*, vol. 8, no. 4, pp. 443–453, Jul. 2000.

[2] A. Spriet, S. Doclo, M. Moonen, and J. Wouters, "Feedback control in hearing aids," in *Springer Handbook Speech Process.* New York, NY, USA: Springer, 2008, pp. 979–1000.

[3] T. van Waterschoot and M. Moonen, "Fifty Years of Acoustic Feedback Control: State of the Art and Future Challenges," *Proc. IEEE*, vol. 99, no. 2, pp. 288–327, Feb. 2011.

[4] J. Hellgren and U. Forssell, "Bias of feedback cancellation algorithms in hearing aids based on direct closed loop identification," *IEEE Trans. Speech Audio Process.*, vol. 9, no. 8, pp. 906–913, Nov. 2001.

[5] S. Laugesen, K. Hansen, and J. Hellgren, "Acceptable delays in hearing aids and implications for feedback cancellation," *J. Acoust. Soc. Amer.*, vol. 105, no. 2, pp. 1211–1212, 1999.

[6] M. Schroeder, "Improvement of acoustic-feedback stability by frequency shifting," *J. Acoust. Soc. Amer.*, vol. 36, no. 9, pp. 1718–1724, 1964.

[7] F. Strasser and H. Puder, "Adaptive feedback cancellation for realistic hearing aid applications," *IEEE/ACM Trans. Audio, Speech, Lang. Process.*, vol. 23, no. 12, pp. 2322–2333, Dec. 2015.

[8] M. Guo, S. H. Jensen, J. Jensen, and S. L. Grant, "On the use of a phase modulation method for decorrelation in acoustic feedback cancellation," in *Proc. 20th Eur. Signal Process. Conf.*, 2012, pp. 2000–2004.

[9] J. Kates, "Feedback cancellation in hearing aids," in *Proc. IEEE Int. Conf. Acoust., Speech, Signal Process.*, 1990, pp. 1125–1128.

[10] M. Guo, S. H. Jensen, and J. Jensen, "Novel acoustic feedback cancellation approaches in hearing aid applications using probe noise and probe noise enhancement," *IEEE Trans. Audio, Speech, Lang. Process.*, vol. 20, no. 9, pp. 2549–2563, 2012.

[11] M. Guo, T. B. Elmedyb, S. H. Jensen, and J. Jensen, "On acoustic feedback cancellation using probe noise in multiple-microphone and single-loudspeaker systems," *IEEE Signal Process. Lett.*, vol. 19, no. 5, pp. 283–286, May 2012.

[12] C. R. C. Nakagawa, S. Nordholm, and W.-Y. Yan, "Feedback cancellation with probe shaping compensation," *IEEE Signal Process. Lett.*, vol. 21, no. 3, pp. 365–369, Mar. 2014.

[13] J. Hellgren, "Analysis of feedback cancellation in hearing aids with filtered-X LMS and the direct method of closed loop identification," *IEEE Trans. Speech Audio Process.*, vol. 10, no. 2, pp. 119–131, Feb. 2002.

[14] A. Spriet, I. Proudler, M. Moonen, and J. Wouters, "Adaptive feedback cancellation in hearing aids with linear prediction of the desired signal," *IEEE Trans. Signal Process.*, vol. 53, no. 10, pp. 3749–3763, Oct. 2005.

[15] G. Rombouts, T. Van Waterschoot, and M. Moonen, "Robust and efficient implementation of the PEM-AFROW algorithm for acousic feedback cancellation," *J. Audio Eng. Soc.*, vol. 55, no. 11, pp. 955–966, 2007.

[16] J. M. Gil-Cacho, T. van Waterschoot, M. Moonen, and S. H. Jensen, "Transform domain prediction error method for improved acoustic echo and feedback cancellation," in *Proc. IEEE 20th Eur. Signal Process. Conf.*, 2012, pp. 2422–2426.

[17] L. T. T. Tran, H. H. Dam, and S. Nordholm, "Affine projection algorithm for acoustic feedback cancellation using prediction error method in hearing aids," in *Proc. IEEE Int. Workshop Acoust. Signal Enhancement*, 2016, pp. 1–5.

[18] L. T. T. Tran, H. Schepker, S. Doclo, H. H. Dam, and S. Nordholm, "Improved practical variable step-size algorithm for adaptive feedback control in hearing aids," in *Proc. IEEE 10th Int. Conf. Signal Process. Commun. Syst.*, 2016, pp. 1–8.

[19] L. T. T. Tran, H. Schepker, S. Doclo, H. H. Dam, and S. Nordholm, "Proportionate NLMS for adaptive feedback control in hearing aids," in *Proc. IEEE Int. Conf. Acoust., Speech Signal Process.*, 2017, pp. 211–215.

[20] A. Spriet, G. Rombouts, M. Moonen, and J. Wouters, "Adaptive feedback cancellation in hearing aids," *Elsevier J. Franklin Inst.*, vol. 343, no. 6, pp. 545–573, 2006.

[21] G. Bernardi, T. van Waterschoot, J. Wouters, and M. Moonen, "An all-frequency-domain adaptive filter with PEM-based decorrelation for acoustic feedback control," in *Proc. IEEE Workshop Appl. Signal Process. Audio Acoust.*, 2015, pp. 1–5.

[22] H. Schepker, L. T. T. Tran, S. Nordholm, and S. Doclo, "Improving adaptive feedback cancellation in hearing aids using an affine combination of filters," in *Proc. IEEE Int. Conf. Acoust., Speech, Signal Process.*, 2016, pp. 231–235.

[23] G. Bernardi, T. van Waterschoot, J. Wouters, M. Hillbratt, and M. Moonen, "A PEM-based frequency-domain Kalman filter for adaptive feedback cancellation," in *Proc. IEEE 23rd Eur. Signal Process. Conf.*, 2015, pp. 270–274.

[24] G. Rombouts, A. Spriet, and M. Moonen, "Generalized sidelobe canceller based combined acoustic feedback-and noise cancellation," *Signal Process.*, vol. 88, no. 3, pp. 571–581, 2008.

[25] G. Rombouts, T. van Waterschoot, K. Struyve, and M. Moonen, "Acoustic feedback cancellation for long acoustic paths using a nonstationary source model," *IEEE Trans. Signal Process.*, vol. 54, no. 9, pp. 3426–3434, Sep. 2006.

[26] A. Spriet, G. Rombouts, M. Moonen, and J. Wouters, "Combined feedback and noise suppression in hearing aids," *IEEE Trans. Audio, Speech, Lang. Process.*, vol. 15, no. 6, pp. 1777–1790, Aug. 2007.

[27] M. Guo, T. B. Elmedyb, S. H. Jensen, and J. Jensen, "Analysis of acoustic feedback/echo cancellation in multiple-microphone and single-loudspeaker systems using a power transfer function method," *IEEE Trans. Signal Process.*, vol. 59, no. 12, pp. 5774–5788, Dec. 2011.

[28] H. Schepker, L. T. T. Tran, S. Nordholm, and S. Doclo, "Acoustic feedback cancellation for a multi-microphone earpiece based on a null-steering beamformer," in *Proc. IEEE Int. Workshop Acoust. Signal Enhancement*, 2016, pp. 1–5.

[29] H. Schepker, L. T. T. Tran, S. Nordholm, and S. Doclo, "Null-steering beamformer for acoustic feedback cancellation in a multi-microphone earpiece optimizing the maximum stable gain," in *Proc. IEEE Int. Conf. Acoust., Speech Signal Process.*, 2017, pp. 341–345.

[30] C. R. C. Nakagawa, S. Nordholm, and W.-Y. Yan, "Dual microphone solution for acoustic feedback cancellation for assistive listening," in *Proc. IEEE Int. Conf. Acoust., Speech Signal Process.*, 2012, pp. 149–152.

[31] C. R. C. Nakagawa, S. Nordholm, and W.-Y. Yan, "Analysis of two microphone method for feedback cancellation," *IEEE Signal Process. Lett.*, vol. 22, no. 1, pp. 35–39, Jan. 2015.

[32] C. R. C. Nakagawa, S. Nordholm, F. Albu, and W.-Y. Yan, "Closed-loop feedback cancellation utilizing two microphones and transform domain processing," in *Proc. IEEE Int. Conf. Acoust., Speech, Signal Process.*, 2014, pp. 3645–3649.

[33] L. T. T. Tran, S. Nordholm, H. Dam, W. Yan, and C. Nakagawa, "Acoustic feedback cancellation in hearing aids using two microphones employing variable step size affine projection algorithms," in *Proc. IEEE Int. Conf. Digit. Signal Process.*, 2015, pp. 1191–1195.

[34] F. Albu, R. Nakagawa, and S. Nordholm, "Proportionate algorithms for two-microphone active feedback cancellation," in *Proc. 23rd Eur. Signal Process. Conf.*, 2015, pp. 290–294.

[35] L. T. T. Tran, H. H. Dam, H. Schepker, S. Doclo, and S. E. Nordholm, "Evaluation of two-microphone acoustic feedback cancellation using uniform and non-uniform sub-bands in hearing aids," in *Proc. Asia-Pacific Signal Inf. Process. Assoc. Annu. Summit Conf.*, 2015, pp. 308–313.

[36] J. M. Kates, "Room reverberation effects in hearing aid feedback cancellation," *J. Acoust. Soc. Amer.*, vol. 109, no. 1, pp. 367–378, 2001.

[37] J. S. Garofolo, "Getting started with the DARPA TIMIT CD-ROM: An acoustic phonetic continuous speech database," vol. 107, Nat. Inst. Standards Technol., Gaithersburgh, MD, USA, 1988.
[38] P. C. Loizou, *Speech Enhancement: Theory and Practice*. Boca Raton, FL, USA: CRC Press, 2013.
[39] J. R. Deller Jr., J. G. Proakis, and J. H. Hansen, *Discrete Time Processing of Speech Signals*. Englewood Cliffs, NJ, USA: Prentice-Hall, 1993.
[40] T. van Waterschoot and M. Moonen, "Adaptive feedback cancellation for audio applications," *Signal Process.*, vol. 89, no. 11, pp. 2185–2201, 2009.
[41] "Method for objective measurements of perceived audio quality," *Int. Telecommun. Union*, Geneva, Switzerland, ITU-R Recommendation BS.1387, 1998.
[42] J. J. Shynk *et al.*, "Frequency-domain and multirate adaptive filtering," *IEEE Signal Process. Mag.*, vol. 9, no. 1, pp. 14–37, Jan. 1992.
[43] A. H. Sayed, *Fundamental Adaptive Filtering*. Hoboken, NJ, USA: Wiley, 2003.

Linh Thi Thuc Tran (S'15) received the B.Eng. degree in electronics and telecommunications from Hanoi University of Technology, Hanoi, Vietnam, in 1999, and the M.Sc. degree in digital communications from the University of Kiel, Kiel, Germany, in 2005. She is currently working toward the Ph.D degree in electrical and computer engineering at Curtin University, Perth, WA, Australia. Her research interests include acoustic feedback control and signal processing, specifically for hearing-aid applications.

Sven Erik Nordholm (SM'04) received the M.Sc. (Civilingenjör) degree in electrical engineering in 1983, the Licentiate degree in engineering in 1989, and the Ph.D. degree in signal processing in 1992, all from Lund University, Lund, Sweden. Since 1999, he is a Professor in signal processing with the Department of Electrical and Computer Engineering, Curtin University, Perth, WA, Australia. From 1999 to 2002, he was the Director of ATRI. From 2002 to 2009, he was the Director in signal processing Laboratory, WATRI, Western Australian Telecommunication Research Institute, a joint institute between The University of Western Australia and Curtin University. He is a co-founder of a start-up companies; Sensear, providing voice communication in extreme noise conditions and Nuheara a hearables company. He is an Associate Editor of the IEEE/ACM TASPL and a member of the IEEE TC AASP. His main research interests include the fields of speech enhancement, adaptive and optimum microphone arrays, audio signal processing and acoustic communication. He has written more than 200 papers in refereed journals and conference proceedings. He contributes frequently in book chapters and encyclopaedia articles and is an Editor of two special issues on hearing aids and microphone arrays. He holds seven patents in the area of speech enhancement and microphone arrays.

Henning Schepker (S'14) received the B.Eng. degree from the Jade University of Applied Sciences, Wilhelmshaven, Germany, in 2011, and the M.Sc. degree (with distinction) from the University of Oldenburg, Oldenburg, Germany, in 2012, both in hearing technology and audiology. He is currently working toward the Ph.D. degree at the Signal Processing Group with the Department of Medical Physics and Acoustics, University of Oldenburg, Oldenburg, Germany. His current work focuses on feedback cancellation for open-fitting hearing aids. His research interests are in the area of signal processing for hearing aids and speech and audio applications as well as speech perception.

Hai Huyen Dam received the Bachelor degree (first class Hons.) and the Ph.D. degree (with distinction) from Curtin University of Technology, Perth, WA, Australia, in 1996 and 2001, respectively. From 1999 to 2000, she spent one year at the Blekinge Institute of Technology, Sweden, as a Researcher. From 2001 to 2007, she was with the Western Australian Telecommunications Research Institute as a Research Fellow and a Senior Research Fellow. Since 2006, she has been a Senior Lecturer with the Department of Mathematics and Statistics, Curtin University, Perth. Her research interests include adaptive array processing, speech enhancement, optimization, equalization, and filter design. She has authored or co-authored more than 40 reviewed journal papers and is a regular reviewer for many conferences and journals.

Simon Doclo (S'95–M'03–SM'13) received the M.Sc. degree in electrical engineering and the Ph.D. degree in applied sciences from the Katholieke Universiteit Leuven, Leuven, Belgium, in 1997 and 2003, respectively. From 2003 to 2007, he was a Postdoctoral Fellow with the Research Foundation Flanders at the Electrical Engineering Department, Katholieke Universiteit Leuven, and the Cognitive Systems Laboratory, McMaster University, Hamilton, ON, Canada. From 2007 to 2009, he was a Principal Scientist with the Sound and Acoustics Group, NXP Semiconductors, Leuven, Belgium. Since 2009, he has been a Full Professor with the University of Oldenburg, Oldenburg, Germany, and a Scientific Advisor for the project group Hearing, Speech and Audio Technology of the Fraunhofer Institute for Digital Media Technology. His research interests include signal processing for acoustical and biomedical applications, more specifically microphone array processing, active noise control, acoustic sensor networks, and hearing aid processing. He was the recipient of the Master Thesis Award of the Royal Flemish Society of Engineers in 1997 (with Erik De Clippel), the Best Student Paper Award at the International Workshop on Acoustic Echo and Noise Control in 2001, the EURASIP Signal Processing Best Paper Award in 2003 (with Marc Moonen), and the IEEE Signal Processing Society 2008 Best Paper Award (with Jingdong Chen, Jacob Benesty, Arden Huang). He is a member of the IEEE Signal Processing Society Technical Committee on Audio and Acoustic Signal Processing, the EURASIP Special Area Team on Acoustic, Speech and Music Signal Processing, and the EAA Technical Committee on Audio Signal Processing. He was the Guest Editor for several special issues (*IEEE Signal Processing Magazine*, *Elsevier Signal Processing*) and is an Associate Editor for the IEEE/ACM TRANSACTIONS ON AUDIO, SPEECH, AND LANGUAGE PROCESSING and EURASIP *Journal on Advances in Signal Processing*.